Responses to Reviewers' Comments on Manuscript acp-2020-398

(Impacts of coagulation on the appearance time method for sub-3nm particle growth rate evaluation and their corrections)

We thank Prof. Dr. Wolfgang Junkermann and the anonymous referee (referred as reviewers #1 and #2 below, respectively) for their efforts and constructive comments that help to improve this manuscript. The reviewer's comments are addressed in the following paragraphs and the manuscript were revised majorly. In response to the concerns of reviewer #1, we clarify in the revised section 3.1 that the numerical models in this study are used to test the proposed formulae rather than investigate the nucleation mechanism in the real atmosphere. The comments are shown as sans-serif dark red texts and our responses are shown as serif black texts. Changes are highlighted in the revised manuscript and shown as "quoted underlined texts" in the responses. Line numbers, figures, and equations quoted in the responses correspond the revised manuscript. References are given at the end of the responses.

Reviewer #1

Summary

The manuscript describes a numerical set of formulas that is used in an aerosol model for the calculation of the growth of aerosol particles after nucleation, especially for the range of ~ 1 nm to 3 nm. This formula set is used for a calculation of the appearance time (time after cluster formation) and later for estimation of the growth rate of the larger sizes aerosols > 4 nm although the main emphasis is on the smallest size ranges, where coagulation has a major effect. Model results based on these formulas are finally compared to a nucleation mode particle event in a relative highly polluted environment in China, in the city of Beijing in a late winter situation.

Response:

This manuscript describes the formulae to correct the influence of coagulation on the appearance time method for growth rate estimation, especially for the range of ~1-3 nm. The derivations of the conventional and corrected appearance time methods for growth rate estimation are detailed in Sections 4.1 and 4.2. In addition to derivations, we also test these formulae for the conventional and corrected appearance time methods using aerosol dynamic models (Section 4.1-4.3, Figs. 1-6). The comparison between the growth rate given by the model and the rates retrieved for the simulated evolution of aerosol size distribution using the conventional and appearance time method support the argument that the impact of coagulation should be corrected when using the appearance time method to estimate the new particle growth rate. Further, we provide an example to illustrate the effect of coagulation on the growth rate retrieved using the appearance time method in the real atmosphere in urban Beijing. A comparison between the growth rates retrieved using the conventional and corrected appearance time method is shown during a new particle formation event in Beijing. There is no comparison between the measured size distributions in urban Beijing and the simulated distributions using the aerosol dynamics models in this study. These research methods are also summarized in the last paragraph of the Introduction section.

According to the reviewer's comments below, a majority of the reviewer's concerns are closely related to the comment "Model results based on these formulas are finally compared to a nucleation mode particle event". Detailed responses will be given following every comment and we present a summary of these responses in the following paragraph.

In the revised manuscript, we clarified that models used in this study are based on aerosol dynamics but not the formulae for conventional or corrected appearance time methods. A paragraph is added at the beginning of Section 3 for

a better understanding. The input of the models are an initial aerosol size distribution and the concentration of the gaseous precursor as a function of time. The evolution of the aerosol size distribution is obtained by solving the aerosol general dynamic equations. Meanwhile, particle growth rate as a function of particle size and time is given by the aerosol dynamic model, which is calculated according to the condensation, evaporation, and coagulation rates. The formulae for conventional or corrected appearance time methods are used to retrieve particle growth rate from the simulated evolution of the aerosol size distribution. Since the simulated growth rate (given by the aerosol dynamic model) is consistent with the simulated evolution of the aerosol size distribution while there are approximations in the estimation using the appearance time methods, the comparison between the simulated growth rate and the growth rate retrieved using the appearance time methods indicates the uncertainty of the appearance time methods in the simulation conditions. The simulation conditions are chosen to elaborate not only the accurateness and uncertainties of the appearance time methods but also the causes of these uncertainties. For instance, Fig. 5 shown the accuracy of the corrected appearance time method under a constant vapor concentration, which support the derivations for the appearance time method. However, since the derivations are based on a constant vapor concentration assumption whereas the vapor concentration in real new particle formation events may vary with time, we present Fig. 6 and Table A1 to shown the uncertainties due to this violation of the constant vapor assumption. After testing the appearance time methods using the aerosol dynamics models, the appearance time methods are applied in a new particle formation event measured in urban Beijing. The growth rate during this event are estimated using the conventional and corrected appearance time methods and their differences indicate the influences of the coagulation on the appearance time of new particles. The measured size distributions and the retrieved growth rates for this new particle formation event are not compared to those given by the aerosol dynamic models.

We revised the first sentence in Section 3.1 as "A discrete aerosol model and a discrete-sectional aerosol model based on aerosol dynamics were used to provide an evolving aerosol size distribution and hence to test the conventional and corrected appearance time methods" and added "Note that the aerosol dynamic models are only used to provide a benchmark to compare the conventional and corrected appearance time methods in this study" at the end of this section.

General comments

The argumentation and description of the formulas seems plausible and is according to the authors in agreement with the theory. Unfortunately this 'reference' theory, which is several times cited in the manuscript, is neither described nor referenced. Also there is no information about this general 'theory' and the underlying nucleation scheme applied. There are several nucleation schemes, binary nucleation of sulfuric acid and water (neutral and ion-assisted), ternary involving sulfuric acid, water, and ammonia; with or without organic species and sulfuric acid or charged sulfuric acid-water-ammonia (Napari et al, 2002; Riccobono et al. 2014; Dunne et al. 2016). Otherwise, the results of the subsequent calculations are at least partially contradicting previous publications that are a base for many 'new particle formation' studies within the last decade.

That discrepancy is likely due to the fact that the calculations are done only with a limited set of condensing substances, likely H_2SO_4. It is well known that the exclusive condensation of H_2SO_4 is too slow for the growth rates observed in the atmosphere and that other substances like VOC's or ELVOC's have a large share on growth rates (Ehn et al, 2014; Kuang et al, 2012; Kupc et al, 2020 and literature cited there). An overview about the problems associated with the investigation of nucleation under Chinese high pollution conditions is given by Chu et al (2019). Here also potential other compounds that might be important for NPF. Cai et al (2017) showed that H_2SO_4 could and should be involved but, high H_2SO_4 concentrations do not necessary lead to particle formation events.

Response: We agree with the reviewer that the nucleation and condensation of a single vapor (e.g., H_2SO_4) is usually insufficient to explain new particle formation in the atmosphere. However, the aim of this study is to investigate how to

estimate the growth rate from the measured aerosol size distributions rather than figure out the compounds contribute to particle growth and the their growth mechanisms. The aerosol dynamic models used to test the formulae of the appearance time methods and they are not used to illustrate the nucleation and growth mechanism. Hence, the simplifications in the aerosol dynamics models in terms of the nucleation mechanism does not affect the tests because they do not affect the consistency between the growth rate and evolution of the aerosol size distribution given by the model. There is no modeling results in the application example in Fig. 7.

A new paragraph was added at the beginning of Section 3 to clarify the reason to use models.

Although it does not influence the statement of the reviewer in this piece of comment, we would like to briefly clarify the conclusion of a previous study (Cai et al., 2017). The reason that high H_2SO_4 concentrations do not necessary lead to particle formation events in urban Beijing is usually because of the aerosol Fuchs surface area concentration (coagulation sink of new particles). When H_2SO_4 concentration was high and coagulation sink was low, there were usually new particles observed in urban Beijing. However, this does not indicate that H_2SO_4 is the only major compound participate new particle formation in urban Beijing and the contributions of other compounds to particle growth were discussion in Cai et al. (2017).

The physical background besides the description of the mathematical steps is largely missing. Neither the environmental conditions for the validity of the model, nor the initial input parameters, temperatures humidity, number and size of large particles acting as a condensation sink etc. are included. 100 nm particles are mentioned in a 'certain' number.

Response: To clarify the background particles used in the aerosol dynamic model, we added "The condensation sink (10^{-3} – 10^{-2} s^{-1}) is contributed simultaneously by a certain number concentration (7.2×10^{2} – 7.2×10^{3} cm^{-3}) of 100 nm background particles and the new particles." Other input parameters (e.g., temperature) are omitted because they does not affect the mathematical derivations and the aerosol dynamics models are only used to test these derivations in this study.

The major difference between the new approach of the 'appearance time method' and the 'old' theory, that needs to be discussed in detail is the result that, for the small particles size the growth rate due to coagulation is slowed down compared to other studies where the growth rate is continuously increasing with size (Kulmala et al, 2004, Kulmala et al, 2013, Kuang et al, 2012). The result is a longer appearance time (12 hour for 4.9 nm) than published elsewhere (Kulmala et al, 2013). For a detailed description of the current understanding of the initial steps of gas to particle conversion, and probably the 'theory' mentioned in the manuscript see also Kulmala et al, 2017 and Yao et al, 2018.

Response: We agree with the reviewer that correcting the effect of coagulation reduces the value of growth rate retrieved using the appearance time method. However, there is no discrepancy of the size dependency of growth rate reported in this study and in previous studies. Figure 7b shows that the growth rate estimated using the corrected appearance time method generally increase with the particle size, while the slightly negative size dependency in the sub-3 nm size range is mainly due to the decreasing H_2SO_4 concentration and the size dependency of the coagulation coefficient.

The apparent relationship between particle growth rate and particle size does not necessarily characterized the size dependency of particle growth rate. In the revised section 2.3, we clarified that "Note that since the appearance time is a function of d_p and GR_{conv} is estimated for difference appearance time, the apparent relationship between GR_{conv} and d_p does not necessarily indicate the size dependency of GR_{conv} at any given moment." For example, the methods in Kulmala et al. (2004, 2013) and this study only provides the growth rate as a function of both particle diameter and its corresponding appearance time. One has to exclude the influence of time-dependent variable (e.g., the varying vapor

concentration) to obtain the size dependency of growth rate. In contrast, Kuang et al. (2012) estimates the size dependency of particle growth rate using a time-and-size-resolved method via solving the aerosol general dynamic equation.

The "longer appearance time (12 hour for 4.9 nm)" refers to Fig. 6, in which the model was used to test the formulae. Hence, the simulated aerosol size distributions in this figure should not be directly compared to the measured size distributions in an atmospheric new particle formation event. Further, the appearance time corresponding to a particle size, by its definition, is a moment rather than a duration. We revised "12 h" as "12:00" to avoid confusion. As shown in Fig. 6, the duration for a particle to grow from 1.0 nm to 4.9 nm is ~2.5 h, which is comparable to the values in previous studies. However, this value is mainly determined by the input H_2SO_4 concentration and it has little contribution to understanding the nucleation mechanism because the models in this study are only used to test the formulae.

The model results are then compared to an event 'typical' for Beijing, with nucleation mode particles observed in late winter (24.2.2018). Also, in this section the authors do not give any details about the environmental conditions at the day of the particle event, nor any detailed information about the location, distance to major roads, height of the aerosol inlet above ground etc.. This information is important in a study about aerosols that may be affected by strong local sources (traffic, home emissions) and potential regional transport. Included is only a reference to a submitted, but still not yet accepted, companion paper. Also, as this is an aerosol study under conditions with a large condensational sink, it would be helpful to have data on fine particle concentration, a 'certain number of 100 nm particles' is way too uncertain.

Response: The example of the new particle formation event in urban Beijing is used to elaborate that under the relatively high coagulation sink in urban Beijing, the influence of coagulation on the appearance time of new particles and hence the retrieved growth rate is non-negligible for sub-3 nm particles. The growth rate estimated using the appearance time method in Fig. 7b was calculated using the measured aerosol size distributions. The measured size distributions in Fig. 7a were not compared to the simulated distributions in Figs. 1-6.

To clarify the environment conditions during this new particle formation event, we added "During 8:00 – 16:00 on this NPF day, the mean temperature, relative humidity, and wind speed are 1.3 °C, 22%, and 1.4 m s^{-1}, respectively" in section 3.2. A recently published manuscript, Deng et al. (2020b), reported the data measured at the same site during the same period. This reference was included to provide detailed information on the measurement site.

The measured aerosol size distribution ranging from 1-400 nm are shown in Fig. 7a. Note that "a certain number of 100 nm" particle were only used in the simulation shown in Figs. 3b – 6, and the simulation was not compared to measurements.

The most important issue, however, is the classification of the experimental comparison data. It is the timing of the event that makes it difficult to match the event with basic atmospheric physics and chemistry and with the current observations that the majority of NPF events are happening during daylight hours. A new particle formation event at that time of the day would require an even faster growth than shown by Kulmala (2013) and not a slower growth as indicated in this manuscript. Both, the 'old' Kulmala 4 hours and the 'new' 12 hours appearance time require nighttime chemistry and physics which has not been reported as a significant source for nucleation.

Response: We have revised "12 h" as "12:00". As shown in Fig. 7a, it took ~2 h for particles at 1.5 nm to grow up to 5 nm during the event on Feb. 24, 2018.

The data presented rather indicate a transport related change of air masses. The H_2SO_4 concentration which is at background levels at sunrise peaks about one hour after sunrise and then steadily declines throughout the day (Fig. 6 of the manuscript). This behavior is contrary to the model where the peak concentration is 4 hours later at noon. This experimental diurnal pattern is neither in agreement with local emissions in a high NO_x environment nor with a photochemical reaction including OH radicals and SO_2.

Response: The H_2SO_4 concentration used in the model (Fig. 6) was an input parameter because the model was used only the test the appearance time method rather than predict the H_2SO_4 concentration. It was determined to be either constant or follow a normal distribution to investigate the influence of a varying vapor concentration on the appearance time method, as detailed in section 4.3.

We agree with the reviewer that transport, mixing, and local emissions may influence the measured H_2SO_4 concentration. However, due to the high condensation sink and hence short atmospheric residence time of H_2SO_4 in the presence of a relatively high aerosol concentration, the measured H_2SO_4 is more likely to form at the observation site than being transported from elsewhere. Figure R1 shows the diurnal variation of SO_2 concentration on Feb. 24, 2018. The steadily decreasing H_2SO_4 concentration in Fig. 7 is in accordance with the decreasing SO_2 concentration between 8:00-16:00, indicating that the photochemical reaction between OH radicals and SO_2 is a major pathway for the formation of H_2SO_4 during this new particle formation event.

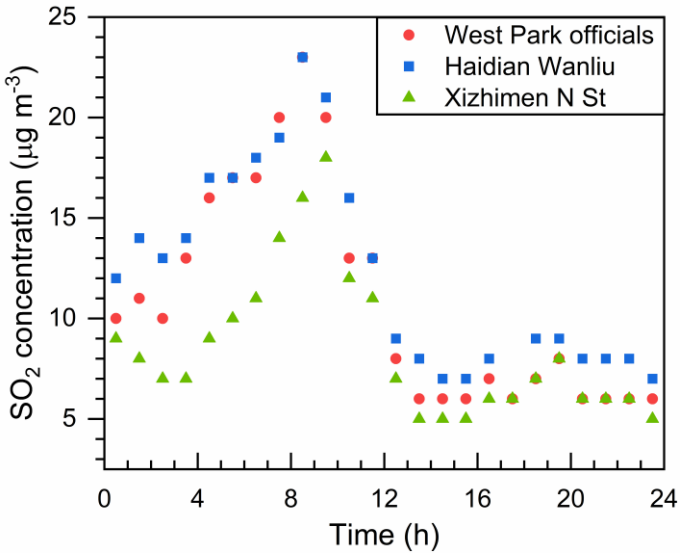

Figure R1. SO_2 concentration measured at three nearest national monitoring stations on Feb. 24, 2018.

Following Kulmala et al (2013) the appearance of 5 nm particles needs about 4 hours after initial cluster formation. This implies for the Beijing case study that cluster formation would occur before sunrise. The air mass at that time has been, according to HYSPLIT, in the area close to the city of Tangshan, not locally in Beijing. Following the results of the current study (appearance time of 4.9 nm particles ~12 hours) clusters would originate even further to the east, close to the coastline at a formation time a few hours after sunset (Fig. 1). This requires a discussion of a nighttime cluster formation chemistry.

Response: As clarified above, Fig. 7a shows that during this new particle formation event, the appearance time for 1.5 nm and 5 nm aerosols are approximately 8:00 and 10:00, respectively. As clarified above, the 12-h growth is a misinterpretation of this manuscript. This appearance time and the measured aerosol size distribution show that new particles down to the cluster size were observed at the site after sunrise and they grew steadily into large particles. Such

a complete formation and growth pattern of new particles indicates a typical regional new particle formation event (Kulmala et al., 2012), although transport, mixing, and local emissions may influence the measured aerosol size distributions.

Along the back trajectories several anthropogenic sources for sulphur compounds are located, that emit a mixture of both, particles and gas phase precursors (Fig. 1). Their emissions include sulfur dioxide, H_2SO_4 (Srivastava et al, 2004) and large amounts of ammonia (Li et al, 2017) and primary nanoparticles produced at elevated temperatures and with or without catalysts, Bai et al, 1992). These are than released into elevated layers of the atmosphere (Junkermann et al, 2011). Measured emission rates of such 'new aerosol generators' are in the order of ~3*10^15 s^{-1} MW^{-1}. Naturally, the emitted particles undergo coagulation and further growth or shrinking (evaporation) depending on the ambient conditions (temperature, humidity) during transport under cool and dry nighttime conditions and the plume conditions favor additional gas to particle conversion (Mohnen and Lodge, 1969). The shape of the diurnal pattern of H_2SO_4 in Beijing is in good agreement with such an advection-convection driven transport, by far better than with a local chemistry initiated cluster formation.

The example of the early morning particle event in Beijing is probably a typical 'nanoparticle' but not a formation event. The experimental verification is looking reasonable but likely does not reflect reality.

Response: We added a paragraph in Section 4.4 on the classification of the observed new particle formation event:

"As shown in Fig. 7, the measured H_2SO_4 concentration started to increase around 7:00 and its 50% appearance time was ~7:30. Because SO_2 concentration declined between 8:00 and 14:00, the peak concentration of H_2SO_4 was observed at 8:00 rather than at noon. Shortly after the increase in H_2SO_4 concentration, new particles down to the cluster size (~1 nm in geometric diameter) was observed. The high concentration of sub-2 nm aerosol during 7:00 - 15:00 and the continuous growth pattern of new particles from 1.5 nm to 10 nm indicates that the observed new particle formation event was a typical regional event (Kulmala et al., 2012), though transport, mixing, and emissions might influence the observed aerosol size distributions."

We disagree with the reviewer's hypothesis that the measured H_2SO_4 and aerosol size distribution at the site were predominated by transport. Due to the short atmospheric residence time of H_2SO_4 and sub-3 nm aerosols (Deng et al, 2020b), it is unlikely that they had been transported from somewhere 150 km away before the detection.

The agreement between the trends of the H_2SO_4 concentration in Fig. 7a and the SO_2 concentration in Fig. R1 supports the hypothesis that the daytime H_2SO_4 during this event was mainly formed by photochemical reaction. The continuous formation and growth pattern of particles down to the cluster size (~1 nm in geometric diameter) shown in Fig. 7a indicates the observed new particle formation event was a typical regional event. Furthermore, the agreement between the 50% appearance time of H_2SO_4 (7:30) and 1.5 nm particles (8:00) in Fig. 7a indicates that the H_2SO_4 formed after sunrise initiates the observed new particle formation event.

The manuscript would need a complete revision due to the missing model and experiment description and not verified nor discussed assumptions about the classification of the particle event. It's also required to discuss the differences between the current model and the previously published growth rate versus particle sizes and the implications on the timing of the whole nucleation process (cluster formation at night versus photochemical reaction).

The authors also should make sure that the appearance of nucleation mode particles in Beijing is applied to a really local phenomena and not to a plume study.

Response: Here we present a summary of revisions in response to the major concerns in the general comments of the reviewer.

- We clarified that the models in this study were used to test the proposed formulae for the appearance time method. There is no comparison between the modeling results and measurements in this study. Besides, we clarified the input background aerosol concentration for the model in the revised manuscript.
- We added more details on the experiments.
- We added a paragraph on the classification of the new particle formation event shown in Fig.7. The continuous formation of aerosols down to the cluster size and their subsequent growth are in accordance with the features of a regional new particle formation event rather than those of a plume event.
- The size-dependency of particle growth rate in the observed new particle formation event is similar to those reported in previous studies.
- The appearance time of H_2SO_4 and new particles on Feb. 24, 2018 indicates that the observed intensive new particle formation was mainly driven by daytime photochemical reaction.

Specific comments:

Model output

The model based on the new formula predicts initially a slow down of the growth rates of new particles within the size range from 1 to 3 nm. The behavior of the growth rates in the 'new' model setup of the manuscript would delay the growth of newly formed particles significantly compared growth rates published elsewhere (Kulmala et al, 2004 and Kulmala et al, 2013). In these publications a continuously increasing growth rate is used. Accordingly, with the new model the growth of new particles to sizes of about 5 nm takes ~10-12 hours compared to 4 hours in the Kulmala et al (2013) example. This is a severe difference likely due to the restriction of only one condensing vapor and has to be discussed in detail because it has strong implications for the time and location of the cluster formation process.

This difference implies several questions that are important for the model – experiment comparison (probably not for the calculation of the impact of coagulation but for the selection of a nucleation event and nocturnal chemistry) that arise, mainly related to timing:

- What is the process producing the initial clusters? At what environmental conditions temperature, RH, radiation?
- Where (locally) does cluster formation happen and, in case, H_2SO_4 is involved, where is its origin?
- Are other compounds required, ammonia, water etc..?
- Why is cluster formation happening at this time and the corresponding chemical reactions are terminated after a few hours while precursors are still present?
- The model is running at least for one version with constant vapor concentration. Is this real?
- When H_2SO_4 is crucial for the cluster formation, why are there no more 5 nm particles appearing 12 hours after the peak of H_2SO_4?
- Why is the assumed H_2SO_4 concentration as high as measured peak values? Within the hours when nucleation mode particles grow in the model from 1 to 3 nm the H_2SO_4 concentration is only a smaller fraction of the model value. H_2SO_4 reaches model values at a time when already 10 nm particles are detected.

Response: As clarified above, the concerns of the reviewer on the aerosol dynamic models and their results are mainly based on misunderstandings of this manuscript. We have revised the manuscript to avoid such confusion.

There is no comparison between the aerosol size distributions and growth rates given by the aerosol dynamic models and obtained from the field campaign in urban Beijing. The models are used to test the formula and they are not based on the formula. Besides, the models are not used to investigate nucleation and growth mechanisms. A continuously increasing

growth rate was observed in this study, which is in accordance with previous literature. It took ~2 h for a 1.5 nm particle to grow up to 5 nm during the observed new particle formation event on Feb. 24, 2018, and this duration of 2 h was estimated from the measured aerosol size distribution rather than predicted by a model.

3D transport:

Looking into the experimental data given in Fig. 7 transport of externally produced particles and precursors is more likely to explain the observations (Cai et al 2018). Transport at night from elevated sources (~300 m) normally happens in clear air (low condensation sink) above the polluted nocturnal surface layer (Fig. 2). Vertical convection mixes rapidly (< 30 min) the air of residual and surface layers in the morning (Platis et al, 2016; Junkermann and Hacker, 2018). Contrary to atmospheric processes industrial nanoparticle sources run 24 hours, seven days a week and include sulphur and nitrogen chemistry as well as ammonia in large amounts (Bai et al, 1992).

A simple budget calculation with a box model similar like in Cai et al (2018) for a 300 km plume originating at Suizhong and Qinhuangdao spreading to ~40 km width (Rosenfeld et al, 2000), assuming a few hundred m residual layer (Platis et al, 2016, Junkermann and Hacker, 2018) and a replacement of the plume volume above Beijing with a wind speed of 25 km h^{-1} results, even without additional new particles, in number concentrations already in the order of magnitude finally observed in Beijing (> 80000 cm^{-3}) and in H_2SO_4 concentrations ~10^8 cm^{-3}, see also Junkermann and Hacker (2018). It is also in agreement with the diurnal pattern (Fig. 6) with convection beginning at ~08:00 local time and downwards mixing of a 200 m layer of this air mass into the low nucleation mode particle concentration 600 m surface layer (HYSPLIT) (Fig. 3). Numbers are based on measured and published emission data for power stations and from HYSPLIT meteorological data along the trajectory and allow at least a rough estimate of the magnitude of concentrations. How far new particle formation plays a role during the dry, cold and dark conditions during the transport and how aerosol size distributions and H_2SO_4 concentrations change would be a perfect task for a complete aerosol-chemistry-transport model. Such a plume production (Mohnen and Lodge, 1969) would widen the nanoparticle size distribution and provide additional particles in the lowest size bins. Field data show, that nighttime transport in the residual layer does not really lead to a massive loss of particles (Fig. 4). The plume hypothesis above is also in agreement with the results of spatial measurements of nucleation mode particles in Germany (Ma and Birmili, 2015) at stations surrounded by several fossil fuel burning power stations using SCR or SNCR technology.

Response: We agree with the reviewer that 3D transport may influence the measured aerosol size distribution and gas concentrations, especially for large (e.g., >5 nm) particles and trace gases with relatively long atmospheric residence time (e.g., SO_2). However, considering the atmospheric residence time of H_2SO_4 and sub-1.5 nm aerosols, the measured data shown in Fig. 7a in this manuscript is most likely a new particle formation event rather than a plume event. Deng et al. (2020b) reported that in urban Beijing, the atmospheric residence time of sub-1.5 nm particles are usually less than 5 min because of the relatively high coagulation sink. Note that there is no coal-fired power plant or cement plant inside the fifth ring road of Beijing. As a result, the observed H_2SO_4 and sub-1.5 nm particles were most likely to be formed near the station via daytime photochemical reactions rather than be transported from kilometers away.

In a perspective from long-term measurements in urban Beijing, the concentration of SO_2 in urban Beijing gradually decreased since 2012 due to strict emission control in northern China. An air pollution prevention and control action plan was conducted since 2013 and it led to a reduction of the $PM_{2.5}$ mass concentration in north China plain by more than 25%. However, the reduction of SO_2 and fine particle emissions and concentrations did not significantly change the frequency of new particle formation events in urban Beijing (Li et al., 2020). Hence, it is unlikely that the new particle formation measured in urban Beijing was often affected by industrial emissions.

In addition to confirming the local formation of new particles using aerosol size spectrometers down to the cluster size, the temporal evolution of the measured size distribution is a key to distinguish new particle formation events from plume events and traffic emissions. The examples given in Iida et al. (2008) show the identification of new particle

formation events in the polluted environment, and similar criterions were also summarized in Kulmala et al. (2012) and Kerminen et al. (2018). Figure R2 shows a plume event measured in urban Beijing. At 10:00, new particles were observed at ~3 nm and these particles grew steadily to ~20 nm at 12:00, which followed the typical pattern of a new particle formation event. However, starting from 14:30, new particles ranging from ~1 nm to ~10 nm with a higher concentration than the existing new particles were observed. Since ~10 nm particles were observed almost simultaneously with ~1 nm particles at 14:30 and there was no clear growth pattern in the measured aerosol size distribution, this event during 14:30 – 17:30 was likely to be a plume event. Note that since new particle down to ~1 nm were observed during this plume event, the source of this plume should be close to rather than away from the sampling site. In contrast, the formation and growth pattern in Fig. 7a indicates that the event observed on Feb. 24, 2018 was a regional new particle formation event.

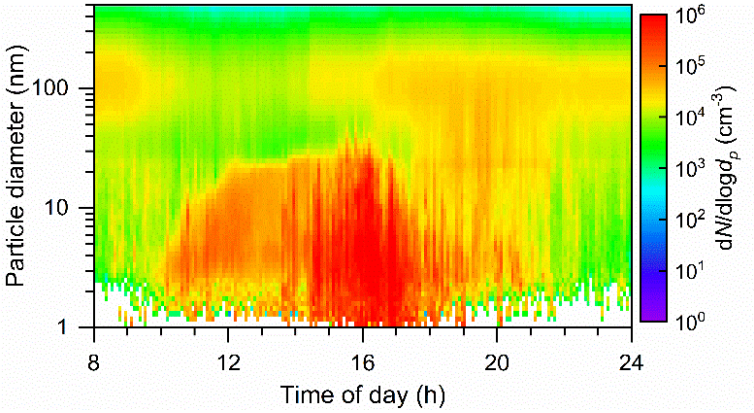

Figure R2. Aerosol size distributions measured in urban Beijing on Apr. 2, 2014.

Minor comments

Who is Julia (Page 7, line 1)

Response: We revised "Julia" as "the Julia programming language". Julia is the name of this programming language.

A reference to a paper under review (Cai et al, 2020) still has to be considered as grey literature as long as the review process is not open access. Also, as it is not clear whether the companion manuscript passes the review process, the information in this other paper is crucial for the current manuscript but might not be available. It could be placed in a supplement.

Response: We replaced Cai et al. (2020) with Deng et al. (2020b). Deng et al. (2020b) has been published and the details on the measurements are detailed therein.

A reference to a paper in preparation (Li and Cai, 2020) is not even grey literature!

Response: Li and Cai (2020) has been published now. The citation information is updated.

Define the conventional method, when it is first cited, Page 5, Lethipalo, 2014? Later in the paper it is confusing, with which model the current results are compared without a reference.

Response: Thanks. We added add a brief description of the conventional appearance time method in Lethipalo et al. (2014).

To clarify the used of the models, we added a paragraph at the beginning of Section 3.The introduction to the models in section 3.1 was revised as "A discrete aerosol model and a discrete-sectional aerosol model based on aerosol dynamics were used to provide an evolving aerosol size distribution and hence to test the conventional and corrected appearance time methods." Li and Cai (2020) is the reference for the discrete-sectional model, which also illustrates the principles of a discrete model. Note that these models were not compared to experiments, because they are used to generate an evolving size distribution rather than to investigate the nucleation and growth mechanism.

The same holds for the theory when the model, which is theory as well, is compared to another theory.

Response: The mechanism for the evolution of aerosol size distribution given by the model was not compared to other nucleation mechanisms. These aerosol dynamics models are used to provide growth rate in consistency with the simulated aerosol size distributions. Since the nucleation and growth mechanism used in these models do not affect this consistency, they do not affect the validity of these models in testing the formulae of the appearance time method. In Fig. 7b, the growth rate retrieved from the measured aerosol size distributions using the appearance time method is compared to the condensational growth rate contributed by H_2SO_4.

Within the time has to be defined in the text and figures. Is this Beijing CST?

Response: Yes. We revised the x-label in Fig. 7a as "Local time (HH:MM)". The time in Figs. 1 and 6 are the simulation time and it does not correspond to the time in a certain day. Hence, we keep the x-labels in Figs. 1 and 6.

Numbering of the tables. Why is the third table named table A1 instead of Table 3?

Response: We intend to put table A1 in the appendix. "A" is short for "appendix".

Reviewer #2

This manuscript investigates the impact of coagulation on the particle growth rate, calculated using the appearance time method, using theoretical derivations and aerosol dynamics modeling. The topic of actual growth rate calculation is of great importance for understanding the new particle formation processes in the atmosphere. The appearance time method was originally developed by Lehtipalo et al., 2014 to calculate growth rate in the size range 1-3nm using PSM data. They highlighted that the method is robust unless coagulation process affect greatly the particles size distributions, such as a heavily polluted environment with high number concentration of preexisting particles. Although this paper is presenting a correction for coagulation on the appearance time method, the approach and the validity of the method are not adequately described. It would be more appropriate to first describe the method and its weaknesses, then present the suggested correction for coagulation impacts and then apply the method in different environment types (boreal forest and Beijing data are available for comparison).These steps, are only briefly described and definitely more examples need to be presented.

Response: We agree with the reviewer that the limitations of the appearance time method should be discussed, though the majority of this manuscript is on the derivation and validation of the correction formula for the appearance time method. The appearance time method is described in the revised Section 2.3. We added section 4.5 on the uncertainties of the appearance time method and the challenges in determining particle growth rate in the atmosphere.

However, we prefer not to extend the scope of this manuscript to applying the appearance time methods to various types of new particle formation events. The impacts of coagulation to the appearance time in the Finnish boreal forest and urban Beijing are indicated in Fig. A1. Meanwhile, as explained in section 4.5, the validation of the appearance time method and other methods in the real atmospheres needs more systematic and comprehensive investigations.

Specific comments:

Page 2, Line 19: Only few or just one application?

Response: According to our knowledge, there is only one published application (Kuang et al., 2012) and some unpublished applications. This sentence was revised as "However, few applications……(e.g., Kuang et al., 2012)" so that is does not emphasize the exact number of applications.

Page 4, Line 13 and 25 and further: Coagulation coefficient unit should be $cm^3\ s^{-1}$.

Response: Thanks. We checked the manuscript and corrected the typos.

Page 5, Line 24: As this paper describes a correction to the appearance time method it is proper to present the method.

Response: Thanks. We added a new paragraph at the beginning of this section to describe the appearance time method.

Page 6, Line 17: This section is lacking all the necessary information for the reader to understand the theoretical and experimental tools that were used to perform this study.

Response: We added a paragraph at the beginning of section 3, which introduces why the simulated and measured new particle formation events are used to test the formulae and what information can be obtained from these test.

Page 7, Line 1: What is Julia?

Response: Julia is a programming language. We replaced "Julia" with "the Julia programming language" in the revised manuscript.

Page 7, Line 20: This reference is a paper under review. More details about the experimental part should be given here.

Response: We added the environmental information on during the presented new particle formation event. The paper under review was replaced by a published paper (Deng et al., 2020b), in which the measurements are detailed.

Page 7, Line 23: This section (4.1) needs to be moved to methods, where the appearance method should be described and cited.

Response: We prefer to keep this section here because this section is mainly on the derivation of the appearance time method under an ideal condition. The derivation itself is a result. Instead, we added a paragraph in 2.3 to introduce the appearance time method and refer to readers to Section 4.1 for more details.

Page 11, Line 14: This is not shown here, we have no indication about sub-1.3nm growth rates.

Response: The reviewer mistook Fig. 5 for Fig. 4. The size range for particle growth rate in Fig. 4 covers 1.0 – 3.5 nm.

Page 11, Line 15:In Figure 4, Coags corrected seems to perform better than the Corrected total growth for particles larger than 3nm.

Response: Yes. This is because the correction term for CoagSrc is an approximation which cannot avoid potential bias. These uncertainties are discussed at the end of Section 4.2. However, considering uncertainties, Fig. 5 (instead of Fig. 4) shows that both the CoagS corrected growth rate and the corrected total growth rate agree with the theoretical growth rate.

Page 11, Line 26: This paragraph is confusing. Which formula is used, Eq 5, or some other formula from the Appendix?

Response: We added "These three impacts of coagulation source are accounted for in the corrected appearance time method (Eqs. 6 and 7)".

Page 12, Line 4: It has to be shown here that the method is described so that all limitations are discussed prior to applying the new method.

Response: The limitation of the correction formulae (Eq. 6) is that the coagulation source term is derivated based on approximation. This limitation has been clarified during the derivation and in this paragraph.

Page 12, Line 13: It is the previous study, or are there more studies?

Response: We added another reference (Olenius et al., 2014) to this sentence.

Page 12, Line 24: I would not use the expression agrees better, as it does not seem to agree, it seems to work better than the conventional method but still overestimates all particle growth rates outside the range 2-3.5 nm. These discrepancies both in absolute values but also with regard to increasing size and especially the shape of the curve have to be discussed further in the text. It has to be noted that the new curve has the same shape as the uncorrected one which suggests that there is an underlying assumption causing these deviations, it is worth providing more information.

Response: We revised this sentence as "the deviation between the corrected particle growth rate and the theoretical growth rate is smaller than the deviation between the conventional growth rate and the theoretical growth rate". The discrepancy outsize the range 2-3.5 nm has been emphasized in the next sentence: "However, for particles larger than ~5 nm and smaller than ~2 nm, the appearance time method overestimates particle growth rate even after correcting the impact of coagulation in the test case." We also added "These overestimations are caused by approximating the influence of coagulation source on particle growth with the coagulation source term in Eq. 5" to illustrate the reason for these discrepancies. In Section 4.2, we have clarified the reason why we use the approximation though it may introduce bias: "Since $CoagSrc_i$ is determined by the concentrations of all particles containing 2 to i-2 molecules, it is difficult to obtain an analytical solution of Eq. 19 without approximation. Here we provide an approximation method to correct the impact of coagulation source to the appearance time."

Page 12, Line 34: This assumption is valid for cases with clear diurnal variations of vapor concentrations as the assumed one. However what happens when condensing species exist in the afternoon as well, then the GR would be much higher. The example in 4.4 is demonstrating this weakness as in the afternoon the GR calculation is three time higher. Sensitivity tests with condensing species not vanishing in the afternoon could be useful as well.

Response: We add "To reduce this systematic bias due to a decreasing vapor concentration…" to emphasize the cause of this bias. If the vapor concentration stays relatively stable after a certain moment, the discrepancy between the theoretical growth rate and the growth rate retrieved using the appearance time method should be smaller. Fig. 5 shows a smaller discrepancy under a constant monomer concertation.

The reviewer misunderstood the example in Section 4.4. In Figs. 2-6, there is a theoretical growth rate given by the model that can be taken as a reference for the retrieved growth rate using the appearance time method. In contrast, the aerosol size distributions in Fig. 7 in Section 4.4 were measured in the real atmosphere and the true growth rate is unknown. Hence, there is no reference growth rate to justify whether the growth rate retrieved using the appearance time method in Fig. 7 is underestimated or overestimated. The condensational growth rate in Fig. 7 was estimated using the measured H_2SO_4 concentration, which is not the true growth rate. We have clarified in Section 4.4 that "Note that the sum of theoretical condensation and coagulation growth rate is not necessarily equal to the theoretical total growth rate for the measured NPF event. This is because only the condensation of sulfuric acid is considered whereas other vapors may also contribute to new particle growth." As a result, condensation of other vapors on the grown particles is more like to be the reason for that the growth rate retrieved using the appearance time method is ~3 times larger than the condensational growth rate calculated using H_2SO_4 concentration. In the main text, we have clarified that "The deviation between the measured growth and theoretical growth for particles larger than ~3 nm indicates that there are other chemical species in addition to sulfuric acid (and the bases to neutralize it) contributing to particle growth."

Page 13, Line 4: A single NPF event is not enough to demonstrate the validity of the proposed correction. Different events, under various meteorological and environmental conditions and under different environment types (and hence condensing species) are necessary to my opinion to test the new formulae.

Response: As clarified in the above response, tests using measured new particle formation events does not validate the proposed formula because the true growth rate is unknown. Instead, the validity and limitations of the proposed formula are tested using the models in the above sections. The aim of this test using a measured new particle formation event is to give an intuitive example of the impacts of coagulation to the appearance time method, though such impacts have been

theoretically predicted in Fig. A1. An example using more new particle formation events is given in Deng et al. (2020a) to shown the comparison between the conventional and appearance time method, yet such a comparison is not a validation.

We added "In addition to the example given in Fig. 7, the average growth rates of 1.5-3 nm particles measured in urban Beijing retrieved using the conventional and corrected appearance time methods were reported in Deng et al. (2020a)." in section 4.4.

We also added a new section 4.5 on the uncertainties of the appearance time method in atmospheric application. As discussed therein, growth rate calculation is usually sensitive to uncertainties. A compressive study including more applications in the atmosphere, comparison between the results retrieved using different methods, and theoretical study based on simulation with uncertainties are needed to figure out a more accurate and robust method for growth rate estimation in the atmosphere.

References

Cai, R., Yang, D., Fu, Y., Wang, X., Li, X., Ma, Y., Hao, J., Zheng, J., and Jiang, J.: Aerosol surface area concentration: a governing factor in new particle formation in Beijing, Atmospheric Chemistry and Physics, 17, 12327-12340, 10.5194/acp-17-12327-2017, 2017.

Deng, C., Cai, R., Yan, C., Zheng, J., and Jiang, J.: Formation and growth of sub-3 nm particles in megacities: impacts of background aerosols, Faraday Discussions, 10.1039/D0FD00083C, 2020a.

Deng, C., Fu, Y., Dada, L., Yan, C., Cai, R., Yang, D., Zhou, Y., Yin, R., Lu, Y., Li, X., Qiao, X., Fan, X., Nie, W., Kontkanen, J., Kangasluoma, J., Chu, B., Ding, A., Kerminen, V., Paasonen, P., Worsnop, R. D., Bianchi, F., Liu, Y., Zheng, J., Wang, L., Kulmala, M., and Jiang, J.: Seasonal characteristics of new particle formation and growth in urban Beijing, Environmental Science and Technology, 54, 8547–8557, 10.1021/acs.est.0c00808, 2020b.

Kenjiro, I., Stolzenburg, M. R., McMurry, P. H., and Smith J. N.: Estimating nanoparticle growth rates from size-dependent charged fractions: Analysis of new particle formation events in Mexico City, J. Geophys. Res., 113, D05207, doi:10.1029/2007JD009260, 2008.

Kuang, C., Chen, M., Zhao, J., Smith, J., McMurry, P. H., and Wang, J.: Size and time-resolved growth rate measurements of 1 to 5 nm freshly formed atmospheric nuclei, Atmospheric Chemistry and Physics, 12, 3573-3589, 10.5194/acp-12-3573-2012, 2012.

Kulmala, M., Vehkamäki, H., Petäjä, T., Dal Maso, M., Lauri, A., Kerminen, V.-M., Birmili, W., and McMurry, P. H.: Formation and growth rates of ultrafine atmospheric particles: a review of observations, Journal of Aerosol Science, 35, 143-176, 10.1016/j.jaerosci.2003.10.003, 2004.

Kulmala, M., Petäjä, T., Nieminen, T., Sipilä, M., Manninen, H. E., Lehtipalo, K., Dal Maso, M., Aalto, P. P., Junninen, H., Paasonen, P., Riipinen, I., Lehtinen, K. E., Laaksonen, A., and Kerminen, V.-M.: Measurement of the nucleation of atmospheric aerosol particles, Nature protocols, 7, 1651-1667, 10.1038/nprot.2012.091, 2012.

Kulmala, M., Kontkanen, J., Junninen, H., Lehtipalo, K., Manninen, H. E., Nieminen, T., Petäjä, T., Sipilä, M., Schobesberger, S., Rantala, P., Franchin, A., Jokinen, T., Jarvinen, E., Äijälä, M., Kangasluoma, J., Hakala, J., Aalto, P. P., Paasonen, P., Mikkilä, J., Vanhanen, J., Aalto, J., Hakola, H., Makkonen, U., Ruuskanen, T., Mauldin, R. L., 3rd, Duplissy, J., Vehkamäki, H., Bäck, J., Kortelainen, A., Riipinen, I., Kurtén, T., Johnston, M. V., Smith, J. N., Ehn, M., Mentel, T. F., Lehtinen, K. E., Laaksonen, A., Kerminen, V.-M., and Worsnop, D. R.: Direct observations of atmospheric aerosol nucleation, Science, 339, 943-946, 10.1126/science.1227385, 2013.

Olenius, T., Riipinen, I., Lehtipalo, K., and Vehkamäki, H.: Growth rates of atmospheric molecular clusters based on appearance times and collision–evaporation fluxes: Growth by monomers, Journal of Aerosol Science, 78, 55-70, 10.1016/j.jaerosci.2014.08.008, 2014.

Impacts of coagulation on the appearance time method for sub-3 nm particle growth rate evaluation and their corrections

Runlong Cai[1,2,*], Chenxi Li[3], Xu-Cheng He[2], Chenjuan Deng[4], Yiqun Lu[5], Rujing Yin[4], Chao Yan[1], Lin Wang[5], Jingkun Jiang[4], Markku Kulmala[1,2], Juha Kangasluoma[1,2]

[1]Aerosol and Haze Laboratory, Beijing Advanced Innovation Center for Soft Matter Science and Engineering, Beijing University of Chemical Technology, 100029 Beijing, China
[2]Institute for Atmospheric and Earth System Research / Physics, Faculty of Science, University of Helsinki, 00014 Helsinki, Finland
[3]School of Environmental Science and Engineering, Shanghai Jiao Tong University, 200240, China
[4]State Key Joint Laboratory of Environment Simulation and Pollution Control, School of Environment, Tsinghua University, 100084 Beijing, China
[5]Shanghai Key Laboratory of Atmospheric Particle Pollution and Prevention (LAP[3]), Department of Environmental Science and Engineering, Fudan University, Shanghai 200433, China

Correspondence to: Runlong Cai (runlong.cai@helsinki.fi)

Keywords: particle growth rate; coagulation; appearance time; new particle formation; sub-3 nm aerosol, clustering

Abstract. The growth rate of atmospheric new particles is a key parameter that determines their survival probability to become cloud condensation nuclei and hence their impact on the climate. There have been several methods to estimate the new particle growth rate. However, due to the impact of coagulation and measurement uncertainties, it is still challenging to estimate the initial growth rate of sub-3 nm particles, especially in polluted environments with high background aerosol concentrations. In this study, we explore the feasibility of the appearance time method to estimate the growth rate of sub-3 nm particles. The principle of the appearance time method and the impacts of coagulation on the retrieved growth rate are clarified. New formulae in both discrete and continuous spaces are proposed to correct the impacts of coagulation. Aerosol dynamic models are used to test the new formulae. New particle formation in urban Beijing is used to illustrate the importance to consider the impacts of coagulation on sub-3 nm particle growth rate and its calculation. We show that the conventional appearance time method needs to be corrected when the impacts of coagulation sink, coagulation source, and particle coagulation growth are non-negligible compared to the condensation growth. Under the simulation conditions with a constant vapor concentration, the corrected growth rate agrees with the theoretical growth rates. The variation of vapor concentration is found to impact the growth rate obtained with the appearance time method. Under the simulation conditions with a varying vapor concentration, the average bias of the corrected 1.5-3 nm particle growth rate range from 6-44%. During the test new particle formation event in urban Beijing, the corrected condensation growth rate of sub-3 nm particles was in accordance with the growth rate contributed by sulfuric acid condensation, whereas the conventional appearance time method overestimated the condensation growth rate of 1.5 nm particles by 80%.

1 Introduction

New particle formation (NPF) is frequently observed in various atmospheric environments (Kulmala et al., 2004;Kerminen et al., 2018;Nieminen et al., 2018;Lee et al., 2019). It contributes significantly to the number concentrations of aerosol and cloud condensation nuclei (CCN) and hence impacts the global climate (Kuang et al., 2009;Kerminen et al., 2012). New particle growth rate is one of the key parameters to characterize NPF events. On the one hand, the newly formed particles (~1 nm) have to survive from coagulation scavenging before they grow to the CCN size (~100 nm). Given the same background aerosol concentration, i.e., the same coagulation loss rate, it is the growth rate that determines the survival probability of new particles (Weber et al., 1997;Lehtinen et al., 2007). Therefore, measuring new particle growth rate accurately contributes to understanding the impact of NPF on the climate. On the other hand, particle growth rate is a key to investigate the growth mechanisms. Theoretical particle growth rates contributed by condensing vapors are usually compared to measured growth rates to reveal the possible particle growth mechanisms (Ehn et al., 2014;Yao et al., 2018;Mohr et al., 2019). A non-biased and accurate determination of measured growth rates is an important fundament of these comparisons.

Although new particle growth rates are frequently reported in various environments around the world, it remains difficult to retrieve accurate particle growth rates from an ambient dataset. Due to the varying atmospheric conditions, significant Kelvin effect, and size-dependent particle compositions, particle growth rate is a function of both time and particle size. The measured evolution of aerosol size distribution does not directly indicate the size-and-time-resolved growth rate of single particles because one cannot directly track single particles from the size distributions. There are several methods to obtain the size-and-time resolved growth rate by solving aerosol general dynamic equations (GDE, Kuang et al., 2012;Pichelstorfer et al., 2018). However, few applications of these GDE methods have been reported for particle growth analysis in the real atmosphere (e.g., Kuang et al., 2012). The most likely reason is that these GDE methods are sensitive to measurement uncertainties caused by atmospheric instability and instruments, which needs to be solved in future studies.

Apart from solving the GDEs, the widely used methods to estimate particle growth rate are based on finding the representing particle diameter or time. The representing diameter method usually uses the peak diameter of the size distribution of new particles and estimates its increase rate from its temporal evolution. The rate of increase of peak diameter is then taken as particle growth rate (Kulmala et al., 2012) after correcting (or sometimes neglecting) the influence of coagulation on the peak shifting (Stolzenburg et al., 2005). During the correction, coagulation is often classified into innermodal coagulation (self-coagulation) and intermodal coagulation (Anttila et al., 2010;Kerminen et al., 2018). The peak diameter is usually obtained by fitting a lognormal function to the measured aerosol size distribution of new particles. With a distinct peak diameter in the growing particle population, this method is theoretically feasible to estimate new particle formation rates. However, the mode fitting is usually tricky, especially when there is no well-defined mode in the growing distribution, either due to the aerosol distribution itself or the measurement uncertainties.

The representing time method estimates the corresponding time for a series of diameters according to a certain criterion and then calculates the growth rate according to the relationship between the diameters and their corresponding time (Dada et

al., 2020). The corresponding time is determined as the time to reach either the maximum concentration (maximum concentration method, Lehtinen and Kulmala, 2003) or a certain proportion of the maximum concentration (appearance time method, Lehtipalo et al., 2014) of a given particle size bin. Previous studies have tested the appearance time under various modeling conditions. Their results indicate that some appearance time methods can reproduce the theoretical growth rate within acceptable uncertainties under certain test conditions (Lehtipalo et al., 2014) but not under other test conditions (Olenius et al., 2014;Kontkanen et al., 2016;Li and McMurry, 2018). As shown in the Theory section below, the discrepancy is because the slope of particle size against their appearance time usually convolves other information (e.g., coagulation) in addition to particle growth.

Determining the growth rate of sub-3 nm particles is more challenging than that of larger particles. Firstly, there are considerable uncertainties in the measured sub-3 nm aerosol size distributions (Kangasluoma et al., 2020) compared to larger-sized particles (e.g., > 10 nm, Wiedensohler et al., 2012). These uncertainties pose a great challenge to the methods based on solving aerosol general dynamic equations. Secondly, during a typical atmospheric NPF event, the sub-3 nm particle size distribution function usually decreases monotonically with the increasing diameter (Jiang et al., 2011b). As a result, the representing diameter method is usually difficult to cover the sub-3 nm size range. In contrast, despite lacking a clear mathematical understanding of the information convolved in the slope of appearance time against particle diameter, the appearance time method is usually favored for sub-3 nm particles and clusters because of the existence of the concentration peak of new particles during an atmospheric NPF event. In addition, the appearance time method is not significantly affected by the systematic instrumental uncertainties because the appearance time of each size bin is only determined by the relative signal rather than the absolute particle concentration.

Coagulation impacts both particle growth and the growth rate calculation, especially for polluted environments and some chamber studies with high aerosol concentrations. The impact of coagulation on aerosol dynamics has been known since decades ago (e.g., McMurry, 1983). Recent studies discussed the importance of considering coagulation when estimating new particle growth rate (Cai and Jiang, 2017), the influence of transport on measured size distributions (Cai et al., 2018), and primary particle emissions (Kontkanen et al., 2020) under a high aerosol concentration. Similarly, neglecting particle coagulation may cause a bias in the retrieved particle growth rate. Therefore, the coagulation growth has to be considered before investigating the contributions of various condensing vapors to particle growth.

In this study, the feasibility and limitations of the appearance time method are investigated based on theoretical derivations. The impact of coagulation on the retrieved growth rate using the appearance time method is explored and then corrected. Aerosol dynamic models are used to test the conventional and corrected methods. After that, the corrected appearance time method is applied in a typical NPF event in urban Beijing to show the impact of coagulation on growth rate evaluation in the real atmosphere.

2 Theory

2.1 Particle growth rate

Before deriving the formulae for the appearance time method, the definitions of particle growth and coagulation loss have to be clarified to avoid potential misunderstanding. Although widely used in NPF analyses, the exact meanings of these two concepts vary with their applied conditions.

Particle growth rate, by definition, is the rate of increase in particle diameter as a function of time for a given particle. Assuming that there is a sufficient number of particles of the same size and compositions, it is reasonable to neglect the influence of the stochastic effect due to a low particle number and use the expectation of the single-particle growth rate to characterize the growth of the aerosol population with the same size. When there is only one condensing vapor, the formula for the expectation of the single-particle condensation growth rate (referred to as the condensation growth rate below for simplicity) is shown in Eq. 1:

$$\mathrm{GR}_{\mathrm{cond}} = \frac{\Delta d_{\mathrm{p}}}{\Delta t} = \beta_{1,\mathrm{p}} N_1 \cdot \left[\sqrt[3]{\left({d_{\mathrm{p}}}^3 + {d_1}^3 \right)} - d_{\mathrm{p}} \right] \quad (1)$$

where $\mathrm{GR}_{\mathrm{cond}}$ is the condensation growth rate (nm·s^{-1}) that neglects evaporation, d_{p} is particle diameter (nm), t is time (s), d_1 is the diameter of the condensing vapor (nm), $\beta_{1,\mathrm{p}}$ is the coagulation coefficient between d_1 and d_{p} (cm^3·s^{-1}), and N_1 is the vapor concentration (cm^{-3}). Particle evaporation is assumed to be negligible and the particle shape is assumed to be spherical both before and after the growth. Note that Eq. 1 is expressed in the discrete form, i.e., it does not assume a continuum particle size ($d_1 \to 0$). When multiple vapors contribute to particle growth simultaneously, the total condensation growth rate is the sum of the condensation growth rates contributed by every single vapor.

In addition to the condensation of vapors, coagulation also contributes to particle growth. For a given particle with the size of d_{p}, the coagulation with a particle much smaller than d_{p} is usually considered as a contribution to its growth. In contrast, the coagulation with a particle much larger than d_{p} is usually considered as the coagulation loss of particle d_{p}. We follow this convention to distinguish coagulation growth and loss, i.e., particle coagulation with another particle no larger than itself is taken as coagulation growth and otherwise, it is taken as coagulation loss. Hence, the formula for the expectation of single-particle coagulation growth rate (referred to as the coagulation growth rate for simplicity) in the discrete form is:

$$\mathrm{GR}_{\mathrm{coag}} = \sum_{d_{\mathrm{i}}=d_{\mathrm{min}}}^{d_{\mathrm{i}}=d_{\mathrm{p}}} \left\{ \beta_{\mathrm{p,i}} N_{\mathrm{i}} \cdot \left[\sqrt[3]{\left({d_{\mathrm{p}}}^3 + {d_{\mathrm{i}}}^3 \right)} - d_{\mathrm{p}} \right] \right\} \quad (2)$$

where $\mathrm{GR}_{\mathrm{coag}}$ is the coagulation growth rate (nm·s^{-1}), d_{min} is the minimum particle size (nm), $\beta_{\mathrm{p,i}}$ is the coagulation coefficient (cm^3·s^{-1}) between d_{p} and d_{i}, and N_{i} is the concentration (cm^{-3}) of particles with the size d_{i}. Since both condensation and coagulation contribute to particle growth, the total single-particle growth rate is equal to the sum of $\mathrm{GR}_{\mathrm{cond}}$ and $\mathrm{GR}_{\mathrm{coag}}$.

When retrieving particle growth rate from the measured aerosol size distributions, the retrieved growth rate is the apparent growth rate. “Apparent” emphasizes that the method does not necessarily guarantee that the retrieved growth rate is equal to the condensation or total growth rate of a single particle or the investigated aerosol population. When using the representing

diameter method, the retrieved apparent growth rate is the increase rate of the peak diameter and it does not directly characterize the growth of any particle(s). For instance, the coagulation loss rate is a function of particle diameter; as a result, the peak diameter shifts towards larger sizes with time because smaller particles are scavenged faster by coagulation than larger particles. Similarly, other size-dependent processes such as condensation and coagulation growth also cause the shift of peak diameter. As a result, the apparent growth rate sometimes needs to be corrected before taken as the total growth rate or the condensation growth rate (Stolzenburg et al., 2005). When using the representing time method, although the retrieved apparent growth rate is close to the condensation growth rate under some modeling conditions (Lehtipalo et al., 2014), their deviation can be significant under other conditions, on which we elaborate in section 4.

2.2 Coagulation sink and source

For a given particle, its coagulation with another particle can be classified into coagulation growth and coagulation loss as aforementioned. This classification is based on the Lagrangian specification that tracks the growth of a single particle. In contrast, according to the Eulerian specification that focuses on given particle diameters, each coagulation causes a sink of two particles and a source of one new particle with a larger diameter regardless of the particle sizes. Herein, we define the coagulation sink and source as the loss and production rate for particle size bins in the Eulerian specification. According to these definitions, the coagulation of a large particle with another smaller particle is counted as the coagulation sink (in the Eulerian specification) but not as the coagulation loss (in the Lagrangian specification) of the large particle. Following previous studies, we use CoagS (s^{-1}) to represent the sink coefficient (Kulmala et al., 2001) and CoagSrc ($cm^{-3}\cdot s^{-1}$) to represent the production rate due to coagulation (Kuang et al., 2012). Their formulae in the discrete form are given below:

$$\mathrm{CoagS} = \sum_{d_\mathrm{i}=d_\mathrm{min}}^{d_\mathrm{i}=d_\mathrm{max}} \beta_{\mathrm{p,i}} N_\mathrm{i} \tag{3}$$

$$\mathrm{CoagSrc} = \sum_{d_\mathrm{i}=d_\mathrm{min}}^{{d_\mathrm{i}}^3={d_\mathrm{p}}^3-{d_\mathrm{min}}^3} 0.5\beta_{\mathrm{i,j}} N_\mathrm{i} N_\mathrm{j} \tag{4}$$

where d_{max} is the maximum particle diameter (nm); d_j is defined by $d_j^3 = d_p^3 - d_i^3$; N_i and N_j are the concentrations of d_i and d_j, respectively; and other variables have been introduced above. Note that CoagS and CoagSrc are defined differently and their units are also different. Table 1 summarizes the differences between the definitions in the Lagrangian and Eulerian specifications.

Table 1

2.3 Formulae for the new appearance time method

The conventional appearance time method has been detailed in Lehtipalo et al. (2014) and its derivation is given below in section 4.1. Here we briefly describe the procedure to retrieve particle growth rate from the temporal evolution of a measured

aerosol size distribution using the appearance time method. For each aerosol size bin, its corresponding appearance time is determined as the moment that the measured aerosol concentration in this size bin reached 50% or any other given proportion of its maximum concentration during the event. The maximum and half-maximum concentration of this size bin can either be taken from the smoothed temporal evolution of the measured concentration or determined by fitting a sigmoid function to the measured data. The growth rate is then estimated as the slope of the diameter of aerosol size bins versus their corresponding appearance time, i.e.,

$$\mathrm{GR}_{\mathrm{conv}} = \frac{\Delta d_{\mathrm{p}}}{\Delta t} \tag{5}$$

where $\mathrm{GR}_{\mathrm{conv}}$ is the total growth rate (nm·s^{-1}) retrieved by the conventional appearance time method; Δd_{p} (nm) is the size difference between two adjacent measured size bins, and Δt (s) is the time difference of the appearance time of these two size bins. Note that since the appearance time is a function of d_{p} and $\mathrm{GR}_{\mathrm{conv}}$ is estimated for different appearance times, the apparent relationship between $\mathrm{GR}_{\mathrm{conv}}$ and d_{p} does not necessarily indicate the size dependency of $\mathrm{GR}_{\mathrm{conv}}$ at any given moment.

The correction formulae for the appearance time method in the discrete space is:

$$\mathrm{GR}_{\mathrm{corr,tot}} = \mathrm{GR}_{\mathrm{conv}} - \left(\mathrm{CoagS} + \frac{\mathrm{CoagSrc}}{2N_{\mathrm{p}}}\right) \cdot \left[\sqrt[3]{\left({d_{\mathrm{p}}}^3 + {d_1}^3\right)} - d_{\mathrm{p}}\right] \tag{6}$$

$$\mathrm{GR}_{\mathrm{corr,cond}} = \mathrm{GR}_{\mathrm{corr,tot}} - \mathrm{GR}_{\mathrm{coag}} \tag{7}$$

where $\mathrm{GR}_{\mathrm{corr,tot}}$ is the total growth rate (nm·s^{-1}) after correcting the impact of both coagulation sink and source; $\mathrm{GR}_{\mathrm{corr,cond}}$ is the condensation growth rate (nm·s^{-1}) after correction; $\mathrm{GR}_{\mathrm{coag}}$ is the coagulation growth rate (nm·s^{-1}); CoagS (s^{-1}) and CoagSrc (cm^{-3}·s^{-1}) are the coagulation sink and coagulation source term for d_{p}, respectively; N_{p} is the number concentration of particles with the size d_{p} at its appearance time. Note that coagulation growth is corrected in Eq. 7 but not Eq. 6.

When measuring particle size distribution using size spectrometers, the measured distributions are usually reported in a certain number of sectional bins. Therefore, in addition to the formula in the discrete form (Eq. 6), the correction formula for the appearance time in the sectional form is given below:

$$\mathrm{GR}_{\mathrm{corr,tot}} = \mathrm{GR}_{\mathrm{conv}} - \left(\mathrm{CoagS} + \frac{\mathrm{CoagSrc}}{2N_{[d\mathrm{p,l}\ d\mathrm{p,u}]}}\right) \cdot \left[\sqrt[3]{\left({d_{\mathrm{p}}}^3 + {d_1}^3\right)} - d_{\mathrm{p}}\right] \tag{8}$$

$$\mathrm{CoagSrc} = 0.5 \iint\limits_{{d_{\mathrm{p,l}}}^3 \le {d_{\mathrm{i}}}^3 + {d_{\mathrm{j}}}^3 < {d_{\mathrm{p,u}}}^3} \beta_{\mathrm{i,j}} n_{\mathrm{i}} n_{\mathrm{j}} \cdot \mathrm{dlog}d_{\mathrm{i}} \cdot \mathrm{dlog}d_{\mathrm{j}} \tag{9}$$

where $d_{\mathrm{p,u}}$ (nm) and $d_{\mathrm{p,l}}$ (nm) are the upper and lower size limits of a given size bin; d_{p} (nm) is the representative diameter (usually the geometric mean diameter) of this size bin; CoagS is the coagulation sink (s^{-1}) for d_{p}; CoagSrc is the coagulation source term (cm^{-3}·s^{-1}) for the given size bin; $N_{[d\mathrm{p,1}\ d\mathrm{p,u}]}$ is the measured concentration (cm^{-3}) of the size bin [$d_{\mathrm{p,l}}$, $d_{\mathrm{p,u}}$] at t_{p}; d_1 is the diameter (nm) of the condensing vapor; and n_{i} is the aerosol size distribution function (dN_{i}/dlogd_{i}, cm^{-3}, where N_{i} is the cumulative distribution) for the given size d_{i}.

The derivation for Eq. 6 is detailed in sections 4.1 and 4.2. The new and conventional appearance time methods are tested using a discrete-sectional model in section 4.3 and a measured atmospheric NPF event in section 4.4.

3 Methods

The proposed correction formula for the appearance time method (Eqs. 6 and 7) are derived in sections 4.1, 4.2, and A1. To test the validity of the conventional and corrected methods, numerical models are used to simulate an evolving aerosol size distribution and provide the theoretical growth rate according to the input monomer concentration. The growth rate are retrieved from the simulated aerosol size distribution using the conventional and corrected appearance time methods and then compared to the theoretical growth rate. After that, the conventional and corrected appearance time methods are applied to a new particle formation event measured in urban Beijing. The impact of coagulation on the appearance time of new particle and hence growth rates are indicated by the differences between the growth rates retrieved from the measured aerosol size distributions using the conventional and corrected appearance time methods.

3.1 Numerical models

A discrete aerosol model and a discrete-sectional aerosol model based on aerosol dynamics were used to provide an evolving aerosol size distribution and hence to test the conventional and corrected appearance time methods. The discrete model assumed that new particle formation is driven by the nucleation and condensation of a certain single-component condensing vapor. The vapor concentration was set as a constant. Condensation, coagulation, and external loss were considered in this discrete model. The concentrations of particles up to the size of 100 vapor molecules (~3.5 nm) were numerically solved using the Julia programming language. The theoretical condensation and coagulation growth rates were calculated using Eqs. 1 and 2.

The discrete-sectional model was composed of 30 discrete bins (up to 2.2 nm) and 400 sectional bins (up to 230 nm). The vapor concentration was assumed to follow a normal distribution to simulate its diurnal variation in the real atmosphere. A growth enhancement factor as a function a particle size (Kuang et al., 2010) was used to account for the condensation of multiple vapors. A certain concentration of 100 nm particles was used as background particles and their concentration and size were kept constant during each simulation. The discrete-section model was coded in Matlab and it is detailed in Li and Cai (2020).

The simulation conditions for Figs. 1 and 3-6 are summarized in Table 2. The simulations with varying vapor concentration are summarized in Table A1. Note that the aerosol dynamic models are only used to provide a benchmark to compare the conventional and corrected appearance time methods in this study.

Table 2

3.2 Measurements

The NPF event measured on Feb. 24th, 2018, in urban Beijing was used to test the appearance time method. During 8:00 – 16:00 on this NPF day, the mean temperature, relative humidity, and wind speed are 1.3 °C, 22%, and 1.4 m s^{-1}, respectively.

The measurement site locates on the west campus of the Beijing University of Chemical Technology, which is close to the west 3rd-ring road of Beijing. The aerosol size distributions were measured using a homemade particle size distribution system (PSD, Liu et al., 2016) and a homemade diethylene glycol scanning mobility particle spectrometer (Jiang et al., 2011a;DEG-SMPS, Cai et al., 2017) equipped with a core sampling apparatus (Fu et al., 2019). The sulfuric acid monomer and dimer concentrations were measured using a long chemical ionization time-of-flight mass spectrometers (ToF-CIMS, Aerodyne Research Inc., Jokinen et al., 2012). The meteorological data were measured using a local weather station (Vaisala, AWS310). More details on this measurement site and the instruments have been introduced elsewhere (Deng et al., 2020b).

4 Results and discussion

4.1 Appearance time method under ideal conditions

Prior to investigating the impacts of coagulation on the appearance time method, we briefly illustrate the principle of the appearance time method. It can be demonstrated that the appearance time method can retrieve the condensation growth rate under ideal conditions. The ideal conditions are:

- The vapor concentration is constant;
- The initial concentrations of new particles are equal to zero;
- Condensation is the only cause of the change in particle concentrations, i.e., there is no coagulation, evaporation, external loss, etc.;
- The condensation rate (i.e., coagulation rate between vapor and particles) is independent of particle diameter.

Under such ideal conditions, the population balance equation for a particle containing i molecules is:

$$\frac{\mathrm{d}N_\mathrm{i}}{\mathrm{d}t} = -\beta N_1 N_\mathrm{i} + \beta N_1 N_{\mathrm{i}-1} \ (\mathrm{i} > 2) \tag{10}$$

where N_1, $N_{\mathrm{i}-1}$, and N_i are the concentrations (cm^{-3}) of the condensing vapor and particles containing i and i-1 monomer molecules, respectively; t is time (s); β is the coagulation coefficient ($\mathrm{cm}^3\cdot\mathrm{s}^{-1}$) between a vapor molecule and any particle, which is assumed to be independent of the particle size in Eq. 10. For the case i = 2, the last term in Eq. 10 should be modified as $0.5\beta N_1^2$.

Solving the differential equations in Eq. 10 yields the analytical solution for N_i:

$$N_\mathrm{i}(t) = N_{\mathrm{i},\infty} \times \left[1 - e^{-\beta N_1 t} \sum_{k=0}^{i-2} \frac{(\beta N_1 t)^k}{k!}\right] \tag{11}$$

where $N_{\mathrm{i},\infty}$ is the concentration limit (cm^{-3}) of N_i when t approaches infinite ($\mathrm{d}N_\mathrm{i}/\mathrm{d}t = 0$) and it is equal to $0.5\beta N_1^2$ (for i > 1) under these ideal conditions.

Figure 1a shows the concentrations of N_i normalized by dividing by their corresponding $N_{\mathrm{i},\infty}$. It can be seen that the distance between two adjacent concentration curves is approximately a constant though these curves are not parallel. Hence, the appearance time method takes the moment that N_i reaches a certain percentage of its maximum value ($N_{\mathrm{i},\infty}$) as its

representative time. Previous studies indicate that the 50% size-resolved appearance time method which chooses the certain percent as 50% is more robust against non-ideal conditions compared to using the criterion of other percent values (Lehtipalo et al., 2014). As shown in Fig. 2, an approximate solution of t for $N_i(t) = 0.5N_{i,\infty}$ (referred to as t_i) is:

$$t_i \approx \frac{\ln 2 + i}{\beta N_1} \tag{12}$$

Equation 12 indicates that the slope of particle size in terms of its molecule number versus its appearance time is approximately equal to its condensation growth rate, i.e.,

$$\frac{\Delta i}{\Delta t} = \frac{i - (i-1)}{t_i - t_{i-1}} \approx \beta N_1 = GR_{cond,n} \tag{13}$$

where $GR_{cond,n}$ is the condensation growth rate in terms of the molecule number (s^{-1}). The relationship between $GR_{cond,n}$ herein and GR_{cond} in Eq.1 (which is defined with respect to particle diameter) is $GR_{cond} = GR_{cond,n} \times \Delta d_i$, where Δd_i (nm) is the increase of d_i due to the condensation of one vapor molecule.

Figure 1

According to the derivations above, the 50% size-resolved appearance time (referred to as 50% appearance time for short) method can retrieve particle growth rate under the given ideal conditions. The slope of particle size versus the appearance time is approximately equal to the condensation growth rate. That is, this slope is mainly determined by condensation growth under these ideal conditions. Note that Eq. 13 is only valid for the 50% appearance time whereas other thresholds to determine the appearance time may cause systematic bias. This bias comes from the non-parallelism of particle concentration curves (see Fig. 1). As shown in Fig. 2, in this test case, the 5% appearance time method overestimates the growth rate by 15% and the 95% appearance time method underestimates the growth rate by 12%. It should be clarified that since these biases are not huge, it is acceptable to use other thresholds in addition to 50% to reduce the impact of measurement uncertainties in practical applications.

Particle evaporation is assumed to be negligible in the above derivations, yet Fig. 2 indicates that evaporation does not significantly impact the validity of the 50% appearance time method. Assuming a size-independent evaporation rate, E (s^{-1}), t_i is approximately equal to $(\ln 2+i)/(\beta N_1\text{-E})$, which is bigger than that without evaporation. Meanwhile, considering evaporation, the net condensation growth rate is equal to the vapor condensation rate subtracted by particle evaporation rate, i.e., βN_1-E. That is, the increase in appearance time agrees with the decrease in the net condensation growth rate. In practice, particle evaporation rate is usually size dependent due to the significant Kelvin effect. The bias caused by this size dependency of evaporation is similar to that of coagulation, though the size dependency of evaporation rate is usually larger than that of coagulation. In addition, the evaporation gain flux ($cm^{-3}s^{-1}$) of a given particle containing i molecules is determined by N_{i+1} rather than N_i. As a result, the slope of particle size versus the 50% appearance time may deviate from the net condensation growth rate when i is a small value and there is a non-negligible difference between N_{i+1} and N_i.

Figure 2

Note that the equality between the slope of particle size versus the 50% appearance time and the net condensation growth rate holds only under the above ideal conditions. The following derivations and results will show how the slope is affected by coagulation while maintaining the same condensation growth rate.

4.2 The impacts of coagulation and their corrections

We first show the impact of an external sink to the appearance time method. The external sink is herein referred to as the sink due to coagulation with background particles, wall loss, dilution, transport, etc. For the convenience of comparison with Fig. 1a, the external sink is assumed to be temporally independent of particle diameter. The impact of its size dependency will be discussed later. Considering the constant external sink, the population balance equation for N_i is:

$$\frac{dN_i}{dt} = -\beta N_1 N_i - ES N_i + \beta N_1 N_{i-1} \quad (i > 2) \tag{14}$$

where ES is the external sink (s^{-1}) and other variables have been introduced in Eq. 10.

Similarly to Eqs. 11 and 12, the approximate solutions for N_i and its corresponding appearance time (t_i) are:

$$N_i(t) = N_{i\infty} \times \left[1 - e^{-(\beta N_1 + ES)t} \sum_{k=0}^{i-2} \frac{[(\beta N_1 + ES)t]^k}{k!}\right] \tag{15}$$

$$t_i \approx \frac{\ln 2 + i}{\beta N_1 + ES} \tag{16}$$

Equations 15 and 16 indicate that the impact of ES to t_i is mathematically equivalent to vapor condensation (βN_1). In the presence of a non-negligible external sink, the particle concentration will approach its limit faster than the scenario without external sink (Fig. 1b). As a result, the slope of particle diameter versus appearance time is affected by both condensation growth and external sink.

Combining Eqs. 1, 13, and 16, the impact of external sink can be readily corrected. The correction formula is:

$$GR_{EScorr} = GR_{conv} - ES \cdot \left[\sqrt[3]{\left(d_p^{\,3} + d_1^{\,3}\right)} - d_p\right] \tag{17}$$

where GR_{EScorr} is the growth rate ($nm \cdot s^{-1}$) after correcting the external sink, GR_{conv} is the growth rate ($nm \cdot s^{-1}$) retrieved by the conventional appearance time method, and d_1 is the diameter (nm) of the condensing vapor.

As shown in Fig. 3a, with a vapor concentration of 5×10^6 cm^{-3} and an external sink ranging from 1×10^{-3} to 5×10^{-3} s^{-1}, the conventional appearance time method overestimates the condensation growth rate substantially. Such an overestimation caused by mistaking the external sink for condensation growth was also reported in previous studies (Olenius et al., 2014;Li and McMurry, 2018). In contrast, the corrected growth rate agrees well with the theoretical condensation growth rate.

Practically, the coagulation coefficient (β) and ES are functions of the particle diameter. For the convenience of illustration, we use the size-dependent coagulation sink, CoagS, as an example to represent the total particle sink due to coagulation, wall loss, dilution, and transport. Similarly to Eq. 15, the approximate analytical solution for N_i with the size-dependent β and CoagS is:

$$N_{\mathrm{i}}(t) \approx N_{\mathrm{i}\infty} \times \left\{ 1 - e^{-(\beta_{1,\mathrm{i}} N_1 + \mathrm{CoagS_i})t} \sum_{\mathrm{k}=0}^{\mathrm{i}-2} \left[\frac{t^{\mathrm{k}}}{\mathrm{k!}} \prod_{\mathrm{g}=\mathrm{i}-\mathrm{k}+1}^{\mathrm{i}} \left(\beta_{1,\mathrm{g}} N_1 + \mathrm{CoagS_g} \right) \right] \right\} \quad (18)$$

where $\beta_{1,\mathrm{i}}$ (or $\beta_{1,\mathrm{g}}$) is the coagulation coefficient between a vapor molecule and a particle containing i (or g) molecules ($cm^3 \cdot s^{-1}$); $CoagS_i$ (or $CoagS_g$) is the coagulation sink of particles containing i (or g) molecules (s^{-1}); and other variables have been introduced above. Correspondingly, the ES term in Eq. 17 should be replaced with $CoagS_i$ to correct the impact of the size-dependent coagulation sink. When deriving Eq. 18, it is assumed that $\beta_{1,i}N_1$+$CoagS_i$ is close to $\beta_{1,i-1}N_1$+$CoagS_{i-1}$. This approximation is reasonable because both $\beta_{1,i}$ and $CoagS_i$ change gradually with the particle size, yet it introduces minor systematic biases in N_i and its corresponding appearance time.

As shown in Fig. 3b, when $\beta_{1,i}$ and $CoagS_i$ are size-dependent, the corrected appearance time method is still able to reproduce the condensation growth rate. It is assumed that the $CoagS_i$ in Fig. 3b is contributed by only the large background particles. Hence, the $CoagS_i$ in Fig. 3b is estimated from the condensation sink (CS) using an empirical formula (Eq. 8 in Lehtinen et al., 2007), where CS indicates the condensation loss rate of the vapor.

Figure 3

In addition to the coagulation with another background particle, the coagulation between two new particles also contributes to the CoagS of both these two particles. As explained in section 2.2, no matter how small the coagulating particle is, the coagulation between a given particle and any other particle should be accounted for in CoagS. This is because the appearance time method is derived in the Eulerian specification and the CoagS is defined for a certain particle diameter rather than for a certain particle. In contrast, when focusing on the survival probability of new particles (Weber et al., 1997;Lehtinen et al., 2007), CoagS should be calculated in the Lagrangian specification, i.e., only the coagulation with a larger particle that causes particle loss should be accounted for. To emphasize the difference between the two definitions of CoagS, the corrected growth rates using the total (Eulerian) CoagS and the background (Lagrangian) CoagS are compared in Fig. 4. Particle source due to coagulation is not considered in this comparison. A constant concentration of 100 nm particles used as the background particles. The background CoagS refers to the sink due to coagulation with all larger particles, including both the background particles and new particles. The total CoagS is calculated using Eq. 3. Note that due to the contribution of new particles, the total CoagS does not follow a simple decreasing trend with the increasing particle diameter (see Fig. B1 in Cai and Jiang, 2017). Hence, the empirical formula (Lehtinen et al., 2007) to generate a size-dependent CoagS in Fig. 4b should not be used for the total CoagS.

As shown in Fig. 4, the condensation growth rate after correcting the background CoagS is still overestimated. In contrast, the growth rate after correcting the total CoagS agrees with the theoretical growth rate for particles larger than 1.3 nm. For sub-1.3 nm particles, the systematic bias of the growth rate after correcting the total CoagS is mainly caused by the violation of the assumption that $\beta_{1,i}N_1$+$CoagS_i$ is close to $\beta_{1,i-1}N_1$+$CoagS_{i-1}$. The size dependence of particle coagulation coefficient under the influence of new particle coagulation increases with decreasing particle size. For instance, under the test conditions,

($\beta_{1,4}N_1$+CoagS$_4$)/($\beta_{1,3}N_1$+CoagS$_3$) = 1.12 while ($\beta_{1,50}N_1$+CoagS$_{50}$)/($\beta_{1,49}N_1$+CoagS$_{49}$) = 1.01. As a result, the corrected appearance time method still overestimates the growth rate for sub-1.3 nm particles.

Figure 4

In addition to CoagS, the impact of coagulation source on the appearance time also needs correction. Adding the coagulation source term to the population balance equation of N_i yields:

$$\frac{dN_i}{dt} = -\beta_{1,i}N_1N_i - \mathrm{CoagS}_i N_i + \beta_{1,i-1}N_1N_{i-1} + \mathrm{CoagSrc}_i \ (i > 2) \quad (19)$$

$$\mathrm{CoagSrc}_i = 0.5\sum_{k=2}^{i-2}\beta_{k,i-k}N_kN_{i-k} \quad (20)$$

where CoagS$_i$ is the coagulation sink (s^{-1}) corresponding to N_i, CoagSrc$_i$ is the coagulation source term (cm^{-3}·s^{-1}) corresponding to N_i, and other variables have been introduced above.

Since CoagSrc$_i$ is determined by the concentrations of all particles containing 2 to i-2 molecules, it is difficult to obtain an analytical solution of Eq. 19 without approximation. Here we provide an approximation method to correct the impact of coagulation source to the appearance time. Compared to the scenario that there is no coagulation source term in the balance equation (Eq. 19), the coagulation source has three impacts on particle size distribution and particle growth: 1) the coagulation with a smaller particle contributes to particle growth; 2) the coagulation source increases the maximum particle concentrations; 3) the coagulation source shortens the time for particles to reach their maximum concentration.

These three impacts of coagulation source are accounted for in the corrected appearance time method (Eqs. 6 and 7). Impact 1) is corrected using Eq. 7. To correct impacts 2) and 3), we simply assume that CoagSrc$_i$ is a constant during the increasing period of N_i and use the following formulae (see the Appendix for its derivation) to estimate the growth rate. The correction formula has been given in Eq. 6.

The corrected appearance time method was tested under various modeling conditions. As the example in Fig. 5 indicates, the growth rates estimated using the corrected appearance time method agrees with the theoretical growth rates. Equation 5 is able to retrieve the growth rate of sub-3 nm particles unless when coagulation source is a governing reason for the change of particle concentration, i.e., CoagSrc/2N_p is comparable or larger than $\beta_{1,p}N_1$. Under these conditions, CoagSrc may not be a constant and, hence, the approximation of CoagSrc/2N_p may cause bias. Fortunately, CoagSrc usually decreases with the increasing particle size due to the decreasing particle concentration. Furthermore, it will be shown in section 4.4 that CoagSrc does not have a major impact on the apparent growth rate even during an intensive atmospheric NPF event. Hence, we consider Eq. 6 as a rough but sufficient formula to correct the impact of coagulation on the appearance time in the real atmosphere.

Figure 5

4.3 The impact of varying vapor concentration

In the above analysis, the vapor concentration is assumed to be constant over the whole particle growth period. This assumption may be valid for some chamber experiments; however, the vapor concentration usually follows a diurnal pattern in the real

atmosphere. The varying vapor concentration may impact the appearance time and hence the retrieved apparent growth rate. As reported in previous studies (Lehtipalo et al., 2014;Olenius et al., 2014), the retrieved appearance time is sensitive to the variation of vapor concentration. In the presence of coagulation, it is difficult to correct the impact of the varying vapor concentration. Herein, we use the discrete-sectional model to test the uncertainties of the corrected appearance time method under a varying vapor concentration. The vapor concentration is assumed to follow a normal distribution. The condensation sink (10^{-3} – 10^{-2} s^{-1}) is contributed simultaneously by a certain number concentration (7.2×10^{2} – 7.2×10^{3} cm^{-3}) of 100 nm background particles and the new particles. The growth rate is firstly estimated using the 50% size-resolved appearance time method and then corrected using Eq. 8. Since the vapor concentration varies with time, the retrieved growth rate characterizes particle growth at both different diameters and different time instead of the size-dependent growth at a certain moment. To keep in accordance with the appearance time method, the theoretical condensation and coagulation growth rates of each d_p are calculated at its corresponding t_p.

In general, neglecting the variation of the vapor concentration introduces biases to the appearance time method. As the example shown in Fig. 6 (test No. 8 in Table) indicates, the deviation between the corrected particle growth rate and the theoretical growth rate is smaller than the deviation between the conventional growth rate and the theoretical growth rate. However, for particles larger than ~5 nm and smaller than ~2 nm, the appearance time method overestimates particle growth rate even after correcting the impact of coagulation in the test case. These overestimations are caused by approximating the influence of coagulation source on particle growth with the coagulation source term in Eq. 6. As summarized in Table A1, the relative discrepancy depends on the exact conditions. The average discrepancy of the corrected appearance time method for 1.5-3 nm particles ranges from 6% to 44% in the test conditions, which is smaller than that of the conventional method.

Although it is difficult to correct the bias due to the varying vapor concentration, one can try to avoid large uncertainties because the bias seems to follow a certain pattern. Compared to the scenario of an increasing vapor concentration, it is found that the discrepancy between the real and retrieved growth rates are usually larger after the peak time of the vapor concentration. As shown in Fig. 6, the appearance time of ~4.9 nm particles is 12:00 and a substantial discrepancy between the theoretical and retrieved growth rate is observed for particles larger than 4.9 nm. Fortunately, during a typical atmospheric NPF event, new particles usually grow large before the vapor concentration starts to decrease. To reduce this systematic bias due to a decreasing vapor concentration, we suggest using the other methods, e.g., the representing diameter method to estimate particle growth rate when the vapor concentration decreases. For sub-2 nm particles, the appearance time usually convolves other information (e.g., the varying vapor concentration and the size-dependent coagulation coefficient) in addition to particle growth. Hence, one should be cautious about the sub-2 nm size-resolved growth rate.

Figure 6

4.4 Application in atmospheric measurements

A typical intense NPF event measured in urban Beijing is used to test the conventional and corrected appearance time methods. During the event, the peak sulfuric acid concentration was ~6×10^{6} cm^{-3} and the average CS for sulfuric acid was 0.024 s^{-1}. The theoretical condensation and coagulation growth rates are calculated using the measured sulfuric acid concentration and aerosol size distribution, respectively. Particle growth due to the uptake of sulfuric acid dimers is herein accounted for as the condensation growth. Note that the sum of theoretical condensation and coagulation growth rate is not necessarily equal to the theoretical total growth rate for the measured NPF event. This is because only the condensation of

sulfuric acid is considered whereas other vapors may also contribute to new particle growth. The enhancement due to Van der Waals force is considered when calculating the coagulation coefficient (Alam, 1987;Chan and Mozurkewich, 2001;Stolzenburg et al., 2019). The appearance time retrieved from the measured aerosol size distributions was smoothed before estimating the particle growth rate. In addition to the example given in Fig. 7, the average growth rates of 1.5-3 nm particles measured in urban Beijing retrieved using the conventional and corrected appearance time methods were reported in Deng et al. (2020a).

As shown in Fig. 7, the measured H_2SO_4 concentration started to increase around 7:00 and its 50% appearance time was 7:30. Because SO_2 concentration declined between 8:00 and 14:00, the peak concentration of H_2SO_4 was observed at 8:00 rather than at noon. Shortly after the increase in H_2SO_4 concentration, new particles down to the cluster size (~1 nm in geometric diameter) was observed. The high concentration of sub-2 nm aerosol during 7:00 - 15:00 and the continuous growth pattern of new particles from 1.5 nm to 10 nm indicates that the observed new particle formation event was a typical regional event (Kulmala et al., 2012), though transport, mixing, and emissions might influence the observed aerosol size distributions.

The impacts of particle coagulation are non-negligible compared to particle growth and the growth rate calculation in urban Beijing. On one hand, the conventional appearance time method overestimates the particle growth rate for sub-3 nm particles in urban Beijing due to the impact of CoagS. The deviation between the conventional and corrected growth rate decreases with the increasing diameter because CoagS decreases with particle diameter. As illustrated above, the correction for CoagSrc is only an approximation rather than obtained based on solid derivations. However, the negligible impact of CoagSrc on the measured growth rate in urban Beijing indicates that this approximation does not cause significant bias. Different from coagulation growth which is weighted by particle size, the CoagSrc of d_p is only determined by the number concentrations of particles smaller than d_p (and their coagulation coefficient). Even under such an intense NPF event (with the maximum formation rate exceeding 200 $cm^{-3} \cdot s^{-1}$), the new particle concentration is usually much smaller than the vapor concentration due to the high CoagS and possibly cluster evaporation. Hence, it is sometimes acceptable to neglect the CoagSrc/N_p term in Eqs. 6 and 8 to facilitate calculation. On the other hand, the coagulation with smaller particles enhances particle growth and this enhancement increases with the increasing particle size. This emphasizes that during an intensive NPF event with a high new particle concentration, the condensation growth rate contributed by condensing vapors cannot be taken as the total growth rate that determines the survival probability of new particles.

Figure 7

The difference between the measured and theoretical growth rates in Fig. 7 also indicates the growth mechanism of new particles. Considering the uncertainties of the appearance time, the sum of condensation and coagulation flux of sulfuric acid molecules and clusters is approximately equal to the measured particle growth rate for ~3 nm particles, which indicates that sulfuric acid is a governing species that contribute to the initial growth of sub-3 nm particles during the test event. The deviation between the measured growth and theoretical growth for particles larger than ~3 nm indicates that there are other chemical species in addition to sulfuric acid (and the bases to neutralize it) contributing to particle growth. Note that the above discussion is only based on a single case study. Hence, further investigations based on long-term measurements are needed to reveal the growth mechanism in the polluted atmospheric environment.

Summarizing all the analysis above, the growth rate retrieved using the conventional appearance time method may be systematically overestimated due to the impact of coagulation, especially for intensive NPF events in polluted environments. Such an overestimation may be significant for sub-3 nm particles because CoagS increases with the decreasing particle size. In addition, the coagulation growth rate also needs to be corrected before investigating the condensation growth mechanism.

For example, in the test case shown in Fig. 7, the retrieved condensation growth rate of 1.5 nm particles using the conventional appearance time method without correcting the impact of CoagS and the coagulation growth rate is overestimated by 80%. Figure 7 also indicates that the impact of CoagS may be negligible for larger particles and clean environments (see also Fig. A1). However, external sinks (e.g., dilution) may also cause an overestimation of the growth rate retrieved using the appearance time method if they are not properly corrected.

4.5 Uncertainties of the appearance time method

Although the proposed correction formulae for the appearance time method in Eqs. 6 and 7 are validated using simulation results and tested using an atmospheric NPF event, there may be other limitations for determining the appearance time in the atmosphere. Differently from controlled chamber studies (Dada et al., 2020), the uncertainties in atmospheric measurements pose challenges to growth rate estimation. These uncertainties come from instrumental biases, atmospheric turbulence, and the omitted contributions from transport, mixing, and emissions to the measured aerosol size distribution. Since the growth rate is calculated using a differential formula (Eq. 5), it is usually more sensitive to uncertainties than a physical quantity calculated using an integral formula (e.g., CoagS). For instance, the appearance time as a function of particle diameter in Fig. 7 had to be smoothed before calculating the growth rate using Eq. 5; otherwise, the calculated growth rate at some certain size bins would be negative. The applications of other methods to estimate the particle growth rate face the same challenge. As discussed in the Introduction, the appearance time method is used to estimate the sub-3 nm aerosol growth rate because other methods sometimes cannot report a growth rate in this size range. Hence, further investigations concerning the uncertainties are needed for a better estimation of the growth rate in the atmosphere.

5 Conclusions

The impact of coagulation on the particle growth rate retrieved using the appearance time method was investigated based on theoretical derivations and aerosol dynamics modeling. It was found that the often-used 50% size-resolved appearance time method can reproduce the condensation growth rate only under the idealized condition without particle coagulation. When using the appearance time method in the real world, coagulation sink, coagulation source, and coagulation growth need to be considered. Equations 5-9 provide a method in both discrete and sectional forms to correct the impacts of coagulation sink and coagulation source to the appearance time method. The feasibility of the corrected method was verified using discrete and discrete-sectional aerosol models. In addition, the variation of vapor concentration was found to impact the appearance time method. The average uncertainties of the corrected 1.5-3 nm particle growth rate for each NPF event were 6-44% in the test cases, respectively. A typical NPF event measured in urban Beijing was used to show the quantitative impacts of coagulation on the retrieved growth rate. The systematic bias of the conventional appearance time method was observed for sub-3 nm particles due to the uncorrected impact of the coagulation sink. Besides, coagulation growth was non-negligible compared to the growth due to sulfuric acid condensation, which emphasizes the importance to distinguish the condensation and total growth rates. During the test event, the apparent growth rate of 1.5 nm particles retrieved using the conventional method was

80% higher than the corrected condensation growth rate, whereas the corrected condensation growth rate was approximately equal to the theoretical growth rate contributed by sulfuric acid condensation.

Appendix

Table A1

Figure A1

Derivation of Eq. 1

Consider a particle population with a uniform diameter of d_p (nm) and a concentration of N_0. N_0 is assumed to be sufficiently large so that the stochastics in particle growth is negligible. At the initial moment t_0 (s), the mean particle diameter is d_p. During a short time interval dt (s), $\beta_{1,p}N_1N_0$dt particles collide with the condensing vapor with a diameter of d_1, where $\beta_{1,p}$ is the coagulation coefficient (cm^3·s^{-1}) and N_1 is the vapor concentration. Hence, the mean diameter ($\overline{d_p}$) weighted by particle number concentration at the moment t_0+dt is:

$$\overline{d_p}(t_0 + \mathrm{d}t) = \beta_{1,p}N_1\mathrm{d}t\sqrt[3]{{d_p}^3 + {d_1}^3} + \left(1 - \beta_{1,p}N_1\mathrm{d}t\right)d_p \quad \text{(Eq. A1)}$$

Comparing $\overline{d_p}(t_0)$ and $\overline{d_p}(t_0 + \mathrm{d}t)$ yields the condensation growth rate:

$$\mathrm{GR_{cond}} = \frac{\overline{d_p}(t_0 + \mathrm{d}t) - \overline{d_p}(t_0)}{\mathrm{d}t} = \beta_{1,p}N_1 \cdot \left[\sqrt[3]{\left({d_p}^3 + {d_1}^3\right)} - d_p\right] \quad \text{(Eq. A2)}$$

The Taylor series of Eq. A2 is:

$$\mathrm{GR_{cond}} = \frac{\beta_{1,p}N_1{d_1}^3}{3{d_p}^2} + o\left[\beta_{1,p}N_1d_p\left(\frac{d_1}{d_p}\right)^6\right] \quad \text{(Eq. A3)}$$

where $o\left[\beta_{1,p}N_1d_p\left(d_1/d_p\right)^6\right]$ is the Peano form of the remainder. The first term on the right-hand side of Eq. A3 is the formula for particle growth rate in the continuous form and the second term (the remainder) is the difference between the growth rate formula in the continuous and discrete forms (Olenius et al., 2018). When d_p is sufficiently larger than d_1, Eq. A2 is reduced to $\beta_{1,p}N_1{d_1}^3/\left(3{d_p}^2\right)$.

The impacts of coagulation source and their corrections

In this section, we present a derivation for Eq. 6. For the convenience of illustration, particle size and growth rate are characterized using the molecule number rather than particle diameter. Assuming that condensation is the only cause of the change in N_i (Eq. 10), the apparent growth rate is equal to the condensation growth rate, i.e.,

$$\mathrm{GR_{conv}} = \mathrm{GR_{app}}^{(10)} = \beta_{1,i}N_1 \quad \text{(Eq. A4)}$$

where $\mathrm{GR_{app}}^{(10)}$ is the apparent growth rate (s^{-1}) of particles containing i molecules and the superscript (10) indicates the population balance assumption in Eq. 10; $\beta_{1,i}$ is the coagulation coefficient (cm^3·s^{-1}) between a vapor molecule and particle i;

and N_i is the concentration (cm^{-3}) of particle i. N_1 is assumed to be constant. The conventional appearance time method takes GR_{app} as the growth rate (GR_{conv}) without correction. The source and maximum concentration of N_i are given below:

$$\mathrm{Src}^{(10)} = \beta_{1,i-1} N_1 N_{i-1} \quad \text{(Eq. A5)}$$

$$N_{i,\infty}{}^{(10)} = \frac{\beta_{1,i-1} N_{i-1,\infty}{}^{(10)}}{\beta_{1,i}} = \frac{2\beta_{1,i-1} N_{i-1}}{\beta_{1,i}} \quad \text{(Eq. A6)}$$

where Src is the source for N_i; the $N_{i-1,\infty}$ is the maximum concentration of N_{i-1} (at $t \to +\infty$); N_{i-1} is the concentration of particle i-1 at its appearance time, hence, it is equal to 50% of $N_{i-1,\infty}$.

Now we consider the scenario with coagulation sink and coagulation source (Eq. 19). The source and maximum concentration of N_i become:

$$\mathrm{Src}^{(19)} = \beta_{1,i-1} N_1 N_{i-1} + \mathrm{CoagSrc}_i \quad \text{(Eq. A7)}$$

$$N_{i,\infty}{}^{(19)} = \frac{\beta_{1,i-1} N_1 N_{i-1,\infty}{}^{(19)} + \mathrm{CoagSrc}_i}{\beta_{1,i} N_1 + \mathrm{CoagS}_i} = \frac{2\beta_{1,i-1} N_1 N_{i-1} + \mathrm{CoagSrc}_i}{\beta_{1,i} N_1 + \mathrm{CoagS}_i} \quad \text{(Eq. A8)}$$

where CoagS_i is the coagulation sink (s^{-1}) corresponding to N_i; and $\mathrm{CoagSrc}_i$ is the coagulation source term ($cm^{-3} \cdot s^{-1}$) corresponding to N_i.

As illustrated in the main text, CoagS_i and $\mathrm{CoagSrc}_i$ change both Src and $N_{i,\infty}$. The conventional (apparent) growth rate under this scenario can be obtained by approximately accounting for these two aspects, i.e.,

$$\begin{aligned} \mathrm{GR}_{conv} &\approx \beta_{1,i} N_1 \cdot \frac{N_{i,\infty}{}^{(10)}}{N_{i,\infty}{}^{(19)}} \cdot \frac{\mathrm{Src}^{(19)}}{\mathrm{Src}^{(10)}} \\ &= \beta_{1,i} N_1 \cdot \frac{2\beta_{1,i-1} N_1 N_{i-1,app}}{\beta_{1,i} N_1} \Big/ \frac{2\beta_{1,i-1} N_1 N_{i-1,app} + \mathrm{CoagSrc}_i}{\beta_{1,i} N_1 + \mathrm{CoagS}_i} \cdot \frac{\beta_{1,i-1} N_1 N_{i-1,app} + \mathrm{CoagSrc}_i}{\beta_{1,i-1} N_1 N_{i-1,app}} \\ &= \left(\beta_{1,i} N_1 + \mathrm{CoagS}_i\right) \cdot \left(1 + \frac{\mathrm{CoagSrc}_i}{2\beta_{1,i-1} N_1 N_{i-1,app} + \mathrm{CoagSrc}_i}\right) \\ &= \beta_{1,i} N_1 + \mathrm{CoagS}_i + \frac{\mathrm{CoagSrc}_i}{N_{i,\infty}} = \beta_{1,i} N_1 + \mathrm{CoagS}_i + \frac{\mathrm{CoagSrc}_i}{2N_{i,app}} \end{aligned} \quad \text{(Eq. A9)}$$

According to Eq. A6, the correction formula for the condensation growth rate, GR_{cond} is:

$$\mathrm{GR}_{cond} = \mathrm{GR}_{conv} - \mathrm{CoagS}_i - \frac{\mathrm{CoagSrc}_i}{2N_{i,app}} \quad \text{(Eq. A10)}$$

Author contributions. RC, JK, JJ, and MK initialized the study. RC and CL developed the models. RC and X-CH derived the formulae. CD, YL, RY, CY, LW, and JJ performed the measurements and analyzed the data. RC did the simulation and wrote the manuscript with the help of other co-authors.

Code availability. The Julia code for the discrete model is available upon request. The Matlab code for the discrete-sectional model can be found via the link in Li and Cai (2020).

Competing interests. The authors declare that they have no conflict of interest.

Acknowledgments. Financial supports from the Finnish Academy of Science project (332547, 1325656), UHEL 3-year grant (75284132), National Key R&D Program of China (2017YFC0209503), and Samsung $PM_{2.5}$ SRP are appreciated.

References

Alam, M. K.: The Effect of van der Waals and Viscous Forces on Aerosol Coagulation, Aerosol Science and Technology, 6, 41-52, 10.1080/02786828708959118, 1987.

Anttila, T., Kerminen, V.-M., and Lehtinen, K. E. J.: Parameterizing the formation rate of new particles: The effect of nuclei self-coagulation, Journal of Aerosol Science, 41, 621-636, 10.1016/j.jaerosci.2010.04.008, 2010.

Cai, R., Chen, D.-R., Hao, J., and Jiang, J.: A miniature cylindrical differential mobility analyzer for sub-3 nm particle sizing, Journal of Aerosol Science, 106, 111-119, 10.1016/j.jaerosci.2017.01.004, 2017.

Cai, R., and Jiang, J.: A new balance formula to estimate new particle formation rate: reevaluating the effect of coagulation scavenging, Atmospheric Chemistry and Physics, 17, 12659-12675, 10.5194/acp-17-12659-2017, 2017.

Cai, R., Chandra, I., Yang, D., Yao, L., Fu, Y., Li, X., Lu, Y., Luo, L., Hao, J., Ma, Y., Wang, L., Zheng, J., Seto, T., and Jiang, J.: Estimating the influence of transport on aerosol size distributions during new particle formation events, Atmospheric Chemistry and Physics, 18, 16587-16599, 10.5194/acp-18-16587-2018, 2018.

Chan, T. W., and Mozurkewich, M.: Measurement of the coagulation rate constant for sulfuric acid particles as a function of particle size using tandem di!erential mobility analysis, Journal of Aerosol Science, 32, 321-339, 10.1016/S0021-8502(00)00081-1, 2001.

Dada, L., Lehtipalo, K., Kontkanen, J., Nieminen, T., Baalbaki, R., Ahonen, L., Duplissy, J., Yan, C., Chu, B., Petaja, T., Lehtinen, K., Kerminen, V. M., Kulmala, M., and Kangasluoma, J.: Formation and growth of sub-3-nm aerosol particles in experimental chambers, Nature Protocol, 15, 1013-1040, 10.1038/s41596-019-0274-z, 2020.

Dal Maso, M., Kulmala, M., Lehtinen, K. E., Mäkelä, J. M., Aalto, P., and O'Dowd, C. D.: Condensation and coagulation sinks and formation of nucleation mode particles in coastal and boreal forest boundary layers, Journal of Geophysical Research, 107, D19, 10.1029/2001jd001053, 2002.

Deng, C., Cai, R., Yan, C., Zheng, J., and Jiang, J.: Formation and growth of sub-3 nm particles in megacities: impacts of background aerosols, Faraday Discussions, 10.1039/d0fd00083c, 2020a.

Deng, C., Fu, Y., Dada, L., Yan, C., Cai, R., Yang, D., Zhou, Y., Yin, R., Lu, Y., Li, X., Qiao, X., Fan, X., Nie, W., Kontkanen, J., Kangasluoma, J., Chu, B., Ding, A., Kerminen, V., Paasonen, P., Worsnop, R. D., Bianchi, F., Liu, Y., Zheng, J., Wang, L., Kulmala, M., and Jiang, J.: Seasonal characteristics of new particle formation and growth in urban Beijing, Environmental Science and Technology, 54, 8547–8557, 10.1021/acs.est.0c00808, 2020b.

Ehn, M., Thornton, J. A., Kleist, E., Sipila, M., Junninen, H., Pullinen, I., Springer, M., Rubach, F., Tillmann, R., Lee, B., Lopez-Hilfiker, F., Andres, S., Acir, I. H., Rissanen, M., Jokinen, T., Schobesberger, S., Kangasluoma, J., Kontkanen, J., Nieminen, T., Kurten, T., Nielsen, L. B., Jorgensen, S., Kjaergaard, H. G., Canagaratna, M., Maso, M. D., Berndt, T., Petaja, T., Wahner, A., Kerminen, V. M., Kulmala, M., Worsnop, D. R., Wildt, J., and Mentel, T. F.: A large source of low-volatility secondary organic aerosol, Nature, 506, 476-479, 10.1038/nature13032, 2014.

Fu, Y., Xue, M., Cai, R., Kangasluoma, J., and Jiang, J.: Theoretical and experimental analysis of the core sampling method: Reducing diffusional losses in aerosol sampling line, Aerosol Science and Technology, 53, 793-801, 10.1080/02786826.2019.1608354, 2019.

Jiang, J., Chen, M., Kuang, C., Attoui, M., and McMurry, P. H.: Electrical Mobility Spectrometer Using a Diethylene Glycol Condensation Particle Counter for Measurement of Aerosol Size Distributions Down to 1 nm, Aerosol Science and Technology, 45, 510-521, 10.1080/02786826.2010.547538, 2011a.

Jiang, J., Zhao, J., Chen, M., Eisele, F. L., Scheckman, J., Williams, B. J., Kuang, C., and McMurry, P. H.: First Measurements of Neutral Atmospheric Cluster and 1–2 nm Particle Number Size Distributions During Nucleation Events, Aerosol Science and Technology, 45, ii-v, 10.1080/02786826.2010.546817, 2011b.

Jokinen, T., Sipilä, M., Junninen, H., Ehn, M., Lönn, G., Hakala, J., Petäjä, T., Mauldin, R. L., Kulmala, M., and Worsnop, D. R.: Atmospheric sulphuric acid and neutral cluster measurements using CI-APi-TOF, Atmospheric Chemistry and Physics, 12, 4117-4125, 10.5194/acp-12-4117-2012, 2012.

Kangasluoma, J., Cai, R., Jiang, J., Deng, C., Stolzenburg, D., Ahonen, L. R., Chan, T., Fu, Y., Kim, C., Laurila, T. M., Zhou, Y., Dada, L., Sulo, J., Flagan, R. C., Kulmala, M., Petäjä, T., and Lehtinen, K.: Overview of measurements and current instrumentation for 1-10 nm aerosol particle number size distributions, Journal of Aerosol Science, 148, 105584, 10.1016/j.jaerosci.2020.105584, 2020.

Kerminen, V.-M., Paramonov, M., Anttila, T., Riipinen, I., Fountoukis, C., Korhonen, H., Asmi, E., Laakso, L., Lihavainen, H., Swietlicki, E., Svenningsson, B., Asmi, A., Pandis, S. N., Kulmala, M., and Petäjä, T.: Cloud condensation nuclei production associated with atmospheric nucleation: a synthesis based on existing literature and new results, Atmospheric Chemistry and Physics, 12, 12037-12059, 10.5194/acp-12-12037-2012, 2012.

Kerminen, V.-M., Chen, X., Vakkari, V., Petäjä, T., Kulmala, M., and Bianchi, F.: Atmospheric new particle formation and growth: review of field observations, Environmental Research Letters, 13, 10.1088/1748-9326/aadf3c, 2018.

Kontkanen, J., Olenius, T., Lehtipalo, K., Vehkamäki, H., Kulmala, M., and Lehtinen, K. E. J.: Growth of atmospheric clusters involving cluster–cluster collisions: comparison of different growth rate methods, Atmospheric Chemistry and Physics, 16, 5545-5560, 10.5194/acp-16-5545-2016, 2016.

Kontkanen, J., Deng, C., Fu, Y., Dada, L., Zhou, Y., Cai, J., Dällenbach, K. R., Hakala, S., Kokkonen, T. V., Lin, Z., Liu, Y., Wang, Y., Yan, C., Petäjä, T., Jiang, J., Kulmala, M., and Paasonen, P.: Size-resolved particle number emissions in Beijing determined from measured particle size distributions, Atmospheric Chemistry and Physics Discussions, accepted, 10.5194/acp-2020-215, 2020.

Kuang, C., McMurry, P. H., and McCormick, A. V.: Determination of cloud condensation nuclei production from measured new particle formation events, Geophysical Research Letters, 36, L09822, 10.1029/2009gl037584, 2009.

Kuang, C., Riipinen, I., Sihto, S. L., Kulmala, M., McCormick, A. V., and McMurry, P. H.: An improved criterion for new particle formation in diverse atmospheric environments, Atmospheric Chemistry and Physics, 10, 8469-8480, 10.5194/acp-10-8469-2010, 2010.

Kuang, C., Chen, M., Zhao, J., Smith, J., McMurry, P. H., and Wang, J.: Size and time-resolved growth rate measurements of 1 to 5 nm freshly formed atmospheric nuclei, Atmospheric Chemistry and Physics, 12, 3573-3589, 10.5194/acp-12-3573-2012, 2012.

Kulmala, M., Dal Maso, M., Mäkelä, J. M., Pirjola, L., Väkevä, M., Aalto, P., Miikkulainen, P., Hämeri, K., and O'dowd, C. D.: On the formation, growth and composition of nucleation mode particles, Tellus, 53, 479-490, 10.3402/tellusb.v53i4.16622, 2001.

Kulmala, M., Vehkamäki, H., Petäjä, T., Dal Maso, M., Lauri, A., Kerminen, V.-M., Birmili, W., and McMurry, P. H.: Formation and growth rates of ultrafine atmospheric particles: a review of observations, Journal of Aerosol Science, 35, 143-176, 10.1016/j.jaerosci.2003.10.003, 2004.

Kulmala, M., Petäjä, T., Nieminen, T., Sipilä, M., Manninen, H. E., Lehtipalo, K., Dal Maso, M., Aalto, P. P., Junninen, H., Paasonen, P., Riipinen, I., Lehtinen, K. E., Laaksonen, A., and Kerminen, V.-M.: Measurement of the nucleation of atmospheric aerosol particles, Nature protocols, 7, 1651-1667, 10.1038/nprot.2012.091, 2012.

Lee, S.-H., Gordon, H., Yu, H., Lehtipalo, K., Haley, R., Li, Y., and Zhang, R.: New Particle Formation in the Atmosphere: From Molecular Clusters to Global Climate, Journal of Geophysical Research: Atmospheres, 124, 7098-7146, 10.1029/2018jd029356, 2019.

Lehtinen, K. E. J., and Kulmala, M.: A model for particle formation and growth in the atmosphere with molecular resolution in size, Atmospheric Chemistry and Physics, 3, 251-257, 10.5194/acp-3-251-2003, 2003.

Lehtinen, K. E. J., Dal Maso, M., Kulmala, M., and Kerminen, V.-M.: Estimating nucleation rates from apparent particle formation rates and vice versa: Revised formulation of the Kerminen–Kulmala equation, Journal of Aerosol Science, 38, 988-994, 10.1016/j.jaerosci.2007.06.009, 2007.

Lehtipalo, K., Leppä, J., Kontkanen, J., Kangasluoma, J., Franchin, A., Wimmer, D., Schobesberger, S., Junninen, H., Petäjä, T., Sipilä, M., Mikkilä, J., Vanhanen, J., Worsnop, D. R., and Kulmala, M.: Methods for determining particle size distribution and growth rates between 1 and 3 nm using the Particle Size Magnifier, Boreal Environment Research, 19, 215-236, 2014.

Li, C., and McMurry, P. H.: Errors in nanoparticle growth rates inferred from measurements in chemically reacting aerosol systems, Atmospheric Chemistry and Physics, 18, 8979-8993, 10.5194/acp-18-8979-2018, 2018.

Li, C., and Cai, R.: Tutorial: The discrete-sectional method to simulate an evolving aerosol, Journal of Aerosol Science, 150, 105615, 10.1016/j.jaerosci.2020.105615, 2020.

Liu, J., Jiang, J., Zhang, Q., Deng, J., and Hao, J.: A spectrometer for measuring particle size distributions in the range of 3 nm to 10 μm, Frontiers of Environmental Science & Engineering, 10, 63-72, 10.1007/s11783-014-0754-x, 2016.

McMurry, P. H.: New particle formation in the presence of an aerosol: rates, time scales, and sub-0.01 μm size distributions, Journal of Colloid and Interface Science, 95, 72-80, 10.1016/0021-9797(83)90073-5, 1983.

Mohr, C., Thornton, J. A., Heitto, A., Lopez-Hilfiker, F. D., Lutz, A., Riipinen, I., Hong, J., Donahue, N. M., Hallquist, M., Petaja, T., Kulmala, M., and Yli-Juuti, T.: Molecular identification of organic vapors driving atmospheric nanoparticle growth, Nat Commun, 10, 4442, 10.1038/s41467-019-12473-2, 2019.

Nieminen, T., Kerminen, V.-M., Petäjä, T., Aalto, P. P., Arshinov, M., Asmi, E., Baltensperger, U., Beddows, D. C. S., Beukes, J. P., Collins, D., Ding, A., Harrison, R. M., Henzing, B., Hooda, R., Hu, M., Hõrrak, U., Kivekäs, N., Komsaare, K., Krejci, R., Kristensson, A., Laakso, L., Laaksonen, A., Leaitch, W. R., Lihavainen, H., Mihalopoulos, N., Németh, Z., Nie, W., amp, apos, Dowd, C., Salma, I., Sellegri, K., Svenningsson, B., Swietlicki, E., Tunved, P., Ulevicius, V., Vakkari, V., Vana, M., Wiedensohler, A., Wu, Z., Virtanen, A., and Kulmala, M.: Global analysis of continental boundary layer new particle formation based on long-term measurements, Atmospheric Chemistry and Physics, 18, 14737-14756, 10.5194/acp-18-14737-2018, 2018.

Olenius, T., Riipinen, I., Lehtipalo, K., and Vehkamäki, H.: Growth rates of atmospheric molecular clusters based on appearance times and collision–evaporation fluxes: Growth by monomers, Journal of Aerosol Science, 78, 55-70, 10.1016/j.jaerosci.2014.08.008, 2014.

Olenius, T., Pichelstorfer, L., Stolzenburg, D., Winkler, P. M., Lehtinen, K. E. J., and Riipinen, I.: Robust metric for quantifying the importance of stochastic effects on nanoparticle growth, Sci Rep, 8, 14160, 10.1038/s41598-018-32610-z, 2018.

Pichelstorfer, L., Stolzenburg, D., Ortega, J., Karl, T., Kokkola, H., Laakso, A., Lehtinen, K. E. J., Smith, J. N., McMurry, P. H., and Winkler, P. M.: Resolving nanoparticle growth mechanisms from size- and time-dependent growth rate analysis, Atmospheric Chemistry and Physics, 18, 1307-1323, 10.5194/acp-18-1307-2018, 2018.

Stolzenburg, D., Simon, M., Ranjithkumar, A., Kürten, A., Lehtipalo, K., Gordon, H., Nieminen, T., Pichelstorfer, L., He, X.-C., Brilke, S., Xiao, M., Amorim, A., Baalbaki, R., Baccarini, A., Beck, L., Bräkling, S., Caudillo Murillo, L., Chen, D., Chu, B., Dada, L., Dias, A., Dommen, J., Duplissy, J., El Haddad, I., Finkenzeller, H., Fischer, L., Gonzalez Carracedo, L., Heinritzi, M., Kim, C., Koenig, T. K., Kong, W., Lamkaddam, H., Lee, C. P., Leiminger, M., Li, Z., Makhmutov, V., Manninen, H. E., Marie, G., Marten, R., Müller, T., Nie, W., Partoll, E., Petäjä, T., Pfeifer, J., Philippov, M., Rissanen, M. P., Rörup, B., Schobesberger, S., Schuchmann, S., Shen, J., Sipilä, M., Steiner, G., Stozhkov, Y., Tauber, C., Tham, Y. J., Tomé, A., Vazquez-Pufleau, M., Wagner, A. C., Wang, M., Wang, Y., Weber, S. K., Wimmer, D., Wlasits, P. J., Wu, Y., Ye, Q., Zauner-Wieczorek, M., Baltensperger, U., Carslaw, K. S., Curtius, J., Donahue, N. M., Flagan, R. C., Hansel, A., Kulmala, M., Volkamer, R., Kirkby, J., and Winkler, P. M.: Enhanced growth rate of atmospheric particles from sulfuric acid, Atmospheric Chemistry and Physics Discussions, in review, 10.5194/acp-2019-755, 2019.

Stolzenburg, M. R., McMurry, P. H., Sakurai, H., Smith, J. N., Mauldin, R. L., Eisele, F. L., and Clement, C. F.: Growth rates of freshly nucleated atmospheric particles in Atlanta, Journal of Geophysical Research, 110, D22S05, 10.1029/2005jd005935, 2005.

Wang, Z. B., Hu, M., Sun, J. Y., Wu, Z. J., Yue, D. L., Shen, X. J., Zhang, Y. M., Pei, X. Y., Cheng, Y. F., and Wiedensohler, A.: Characteristics of regional new particle formation in urban and regional background environments in the North China Plain, Atmospheric Chemistry and Physics, 13, 12495-12506, 10.5194/acp-13-12495-2013, 2013.

Weber, R. J., Marti, J. J., McMurry, P. H., Eisele, F. L., Tanner, D. J., and Jefferson, A.: Measurements of new particle formation and ultrafine particle growth rates at a clean continental site, Journal of Geophysical Research: Atmospheres, 102, 4375-4385, 10.1029/96jd03656, 1997.

Wiedensohler, A., Birmili, W., Nowak, A., Sonntag, A., Weinhold, K., Merkel, M., Wehner, B., Tuch, T., Pfeifer, S., Fiebig, M., Fjäraa, A. M., Asmi, E., Sellegri, K., Depuy, R., Venzac, H., Villani, P., Laj, P., Aalto, P., Ogren, J. A., Swietlicki, E., Williams, P., Roldin, P., Quincey, P., Hüglin, C., Fierz-Schmidhauser, R., Gysel, M., Weingartner, E., Riccobono, F., Santos, S., Grüning, C., Faloon, K., Beddows, D., Harrison, R., Monahan, C., Jennings, S. G., O'Dowd, C. D., Marinoni, A., Horn, H. G., Keck, L., Jiang, J., Scheckman, J., McMurry, P. H., Deng, Z., Zhao, C. S., Moerman, M., Henzing, B., de Leeuw, G., Löschau, G., and Bastian, S.: Mobility particle size spectrometers: harmonization of technical standards and data structure to facilitate high quality long-term observations of atmospheric particle number size distributions, Atmospheric Measurement Techniques, 5, 657-685, 10.5194/amt-5-657-2012, 2012.

Yao, L., Garmash, O., Bianchi, F., Zheng, J., Yan, C., Kontkanen, J., Junninen, H., Mazon, S. B., Ehn, M., Paasonen, P., Sipilä, M., Wang, M., Wang, X., Xiao, S., Chen, H., Lu, Y., Zhang, B., Wang, D., Fu, Q., Geng, F., Li, L., Wang, H., Qiao, L., Yang, X., Chen, J., Kerminen, V.-M., Petäjä, T., Worsnop, D. R., Kulmala, M., and Wang, L.: Atmospheric new particle formation from sulfuric acid and amines in a Chinese megacity, Science, 361, 278-281, 10.1126/science.aao4839, 2018.

Tables and Figures

Table 1 The impacts of coagulation characterized in the Lagrangian and Eulerian specifications.

	Coagulating with a smaller particle	Coagulating with a larger particle
Lagrangian: tracking individual particles	Coagulation growth (GR_{coag})	Coagulation loss
Eulerian: tracking a given size bin	Coagulation sink (CoagS) for the current bin Coagulation source (CoagSrc) for the next bin	

Table 2 The simulation conditions for Figs. 1 and 3-6. The symbol "√" indicates "yes" and the blank indicates "no".

Figure No.	Constant coagulation coefficient?	External sink?	Coagulation sink?	Coagulation source?	Constant vapor concentration?
1a	√				√
1b & 3a	√	√			√
3b & 4			√		√
5			√	√	√
6			√	√	

Table A1 The mean and maximum relative errors of the conventional and corrected appearance time methods for 1.5-3 nm particles. Conv. and corr. are short for the conventional and corrected methods, respectively. The vapor concentration is assumed to follow a normal distribution with a peak concentration of N_{max} and a standard deviation of σ_t. Background CS characterizes the concentration of 100 nm background particles. The errors are given in relative values. The results of No. 8 test is shown in Fig. 6.

No.	N_{max} (cm^{-3})	σ_t (h)	Background CS (s^{-1})	Mean error conv.	Mean error corr.	Max. error corr.
1	5.0×10^6	2	2×10^{-3}	35%	8%	19%
2	2.0×10^6	2	2×10^{-3}	63%	32%	77%
3	3.5×10^6	2	2×10^{-3}	30%	6%	18%
4	8.0×10^6	2	2×10^{-3}	71%	44%	150%
5	5.0×10^6	1	2×10^{-3}	38%	11%	40%
6	5.0×10^6	3	2×10^{-3}	38%	10%	16%
7	5.0×10^6	4	2×10^{-3}	39%	11%	17%
8	5.0×10^6	2	1×10^{-3}	50%	24%	88%
9	5.0×10^6	2	5×10^{-3}	21%	20%	66%
10	5.0×10^6	2	1×10^{-2}	37%	29%	94%

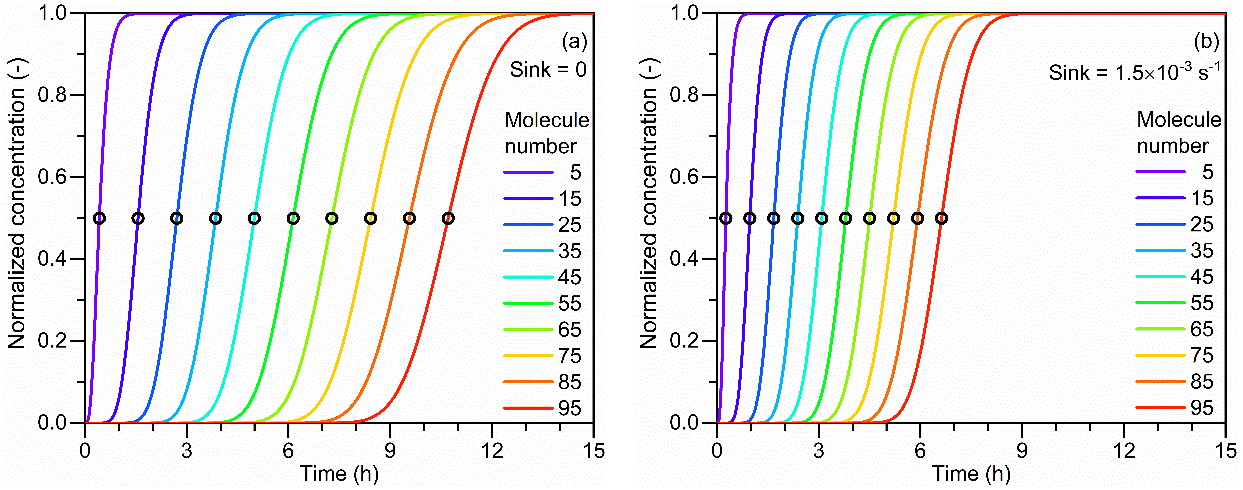

Figure 1 The principle of the appearance time method and the impact of the external sink. (a) Normalized particle concentrations as a function of time. The concentrations are normalized by dividing their corresponding maximum concentrations. The number concentration of the condensation vapor is assumed to be constantly 5×10^{6} cm^{-3}. Particle coagulation sink and other sinks are assumed to be negligible. Particle size is indicated by the molecule number contained in every single particle. The open scatters indicate the 50% appearance time corresponding to each particle size. (b) A constant external sink of 1.5×10^{-3} s^{-1} is considered and other simulation conditions are the same as a). Note that due to the assumption of the size-independent coagulation coefficient, the appearance time in this figure deviates from that in real new particle formation events.

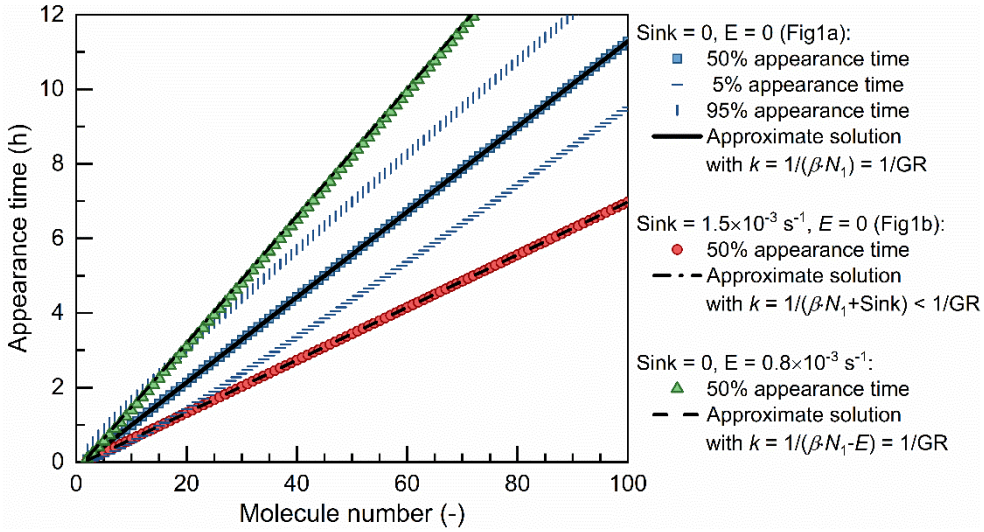

Figure 2 The retrieved appearance time as a function of particle size. The particle size is characterized by the number of molecules contained in each single particle. The scatters are the appearance time retrieved from the simulated concentrations. The curves are the approximate solutions for the 50% appearance time, $t_i = k\times(i+\ln 2)$, where k is the slope of the curve (see Eqs. 7 and 11). β is the coagulation coefficient ($cm^3 \cdot s^{-1}$) between vapor and particles, N_1 is the vapor concentration (5×10^6 cm^{-3}), and E is the particle evaporate rate (s^{-1}). When sink = 0, the slope of the approximate solution is equal to the theoretical net condensation growth rate (GR, in terms of the molecule number contained in every single molecule), βN_1-E. However, when sink > 0, the apparent growth rate, βN_1+Sink, is higher than the theoretical condensation growth rate, βN_1.

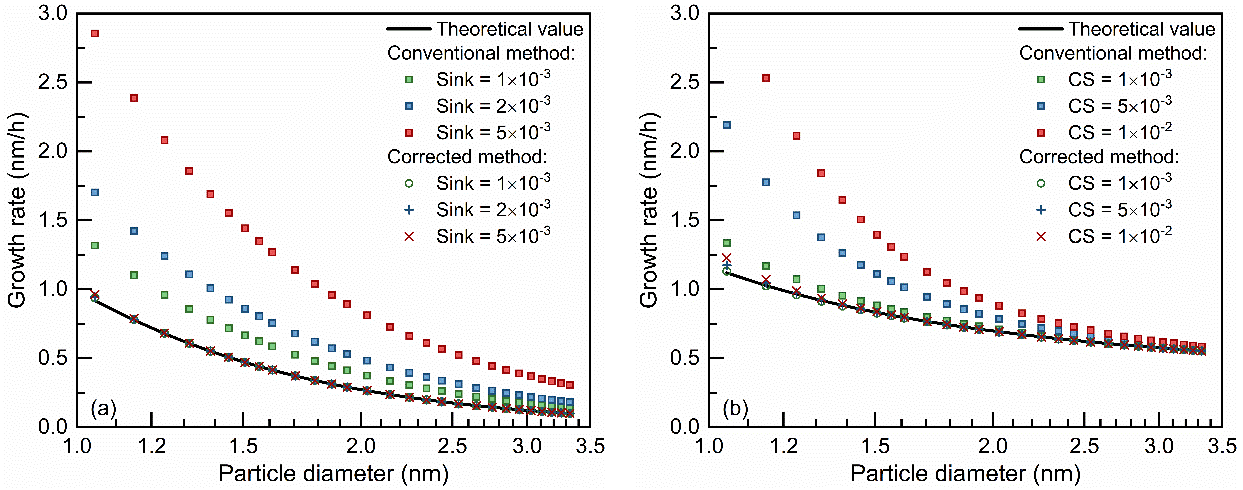

Figure 3 The impact of sinks for the appearance time method and its correction. The theoretical curve is obtained using the condensation rate of the condensing vapor (Eq. 1) and the scatters are obtained using the conventional and corrected appearance time method. The sink is assumed to be independent and dependent of particle diameter in (a) and (b), respectively. The scatters for the corrected method lie on top of each other. The size-dependent coagulation sink in (b) was estimated from the condensation sink (CS) shown in legend using an empirical formula (Lehtinen et al., 2007). The coagulation sink is taken as the input value of the model, hence, the validity of the empirical formula does not affect the accuracy of simulated size distribution or the growth rate. The minor discrepancy among the corrected growth rate comes from the size-dependent particle coagulation coefficient and coagulation sink.

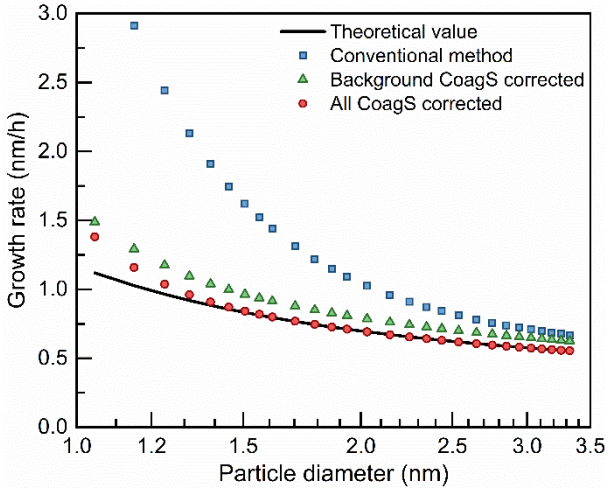

Figure 4 The impact of coagulation sink (CoagS) due to colliding with a smaller particle to the appearance time method. Only the coagulation with a larger particle is accounted for in the correction using the background CoagS.

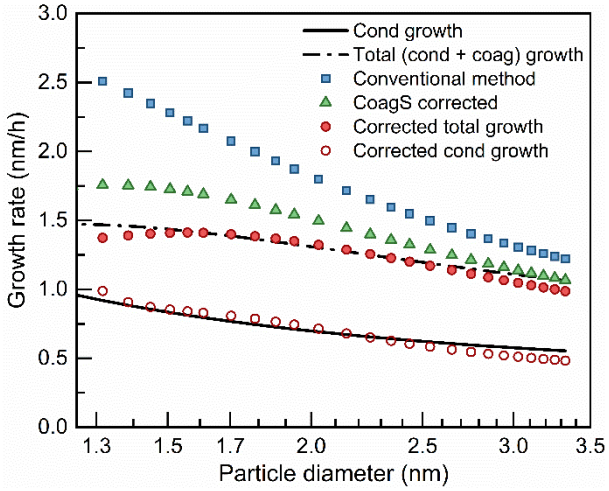

Figure 5 The impact of coagulation sink (CoagS) and coagulation source (CoagSrc) to the appearance time method and the contribution of coagulation growth. Cond and coag are short for condensation and coagulation, respectively. Note that both the solid and dashed lines are theoretical growth rates and their difference is the coagulation growth. Similarly, both the open and filled circles are the measured growth rates after correction and their difference is equal to the coagulation growth rate.

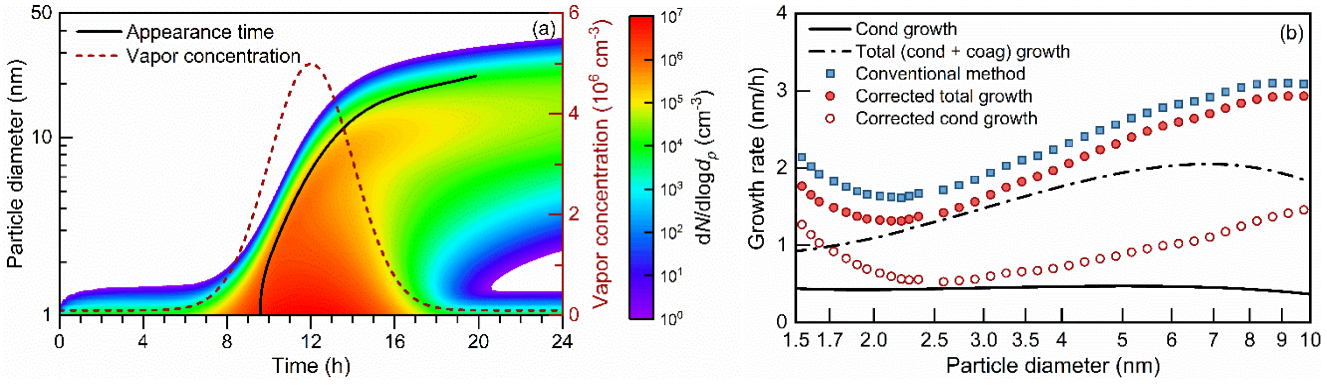

Figure 6 The appearance time method under a varying vapor concentration. The test condition is summarized in Table A1, No. 8. (a) An NPF event simulated using a discrete-sectional aerosol dynamic model. The vapor concentration is assumed to follow a normal distribution (with a background value of 10^5 cm^{-3}). The 100-nm background particles are not shown. The particle diameter as a function of the appearance time is shown in the solid line. (b) The theoretical and retrieved particle growth rates. Cond and coag are short for condensation and coagulation, respectively.

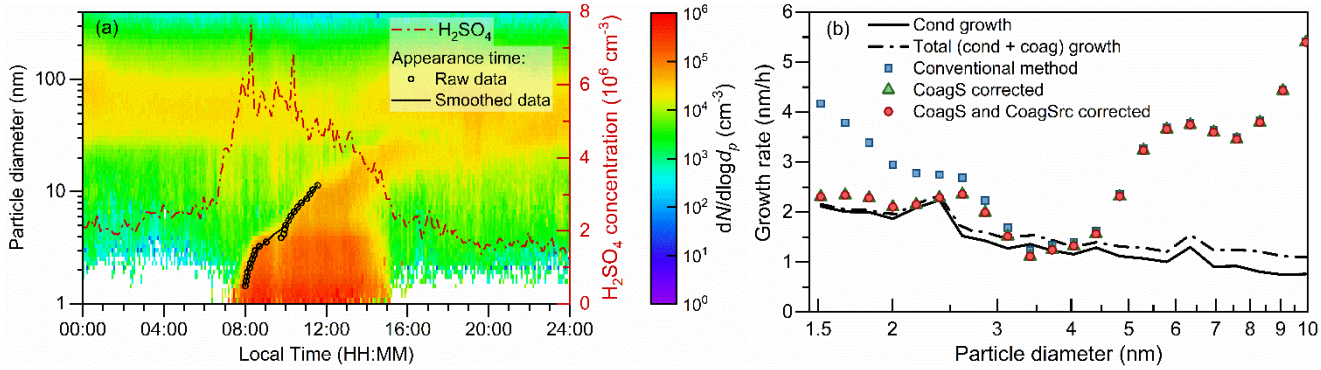

Figure 7 A case study for the appearance time method in the real atmosphere. (a) Aerosol size distribution and H_2SO_4 concentration measured on an NPF day. The event was measured on Feb. 24th, 2018, in urban Beijing. (b) Measured growth rates using the conventional and corrected appearance time methods and the theoretical growth rate contributed by sulfuric acid condensation and particle coagulation. Cond and coag are short for condensation and coagulation, respectively. Note that the theoretical growth rate considers only the sulfuric acid condensation, hence, it may underestimate the overall condensation growth rate contributed by multiple condensing vapors.

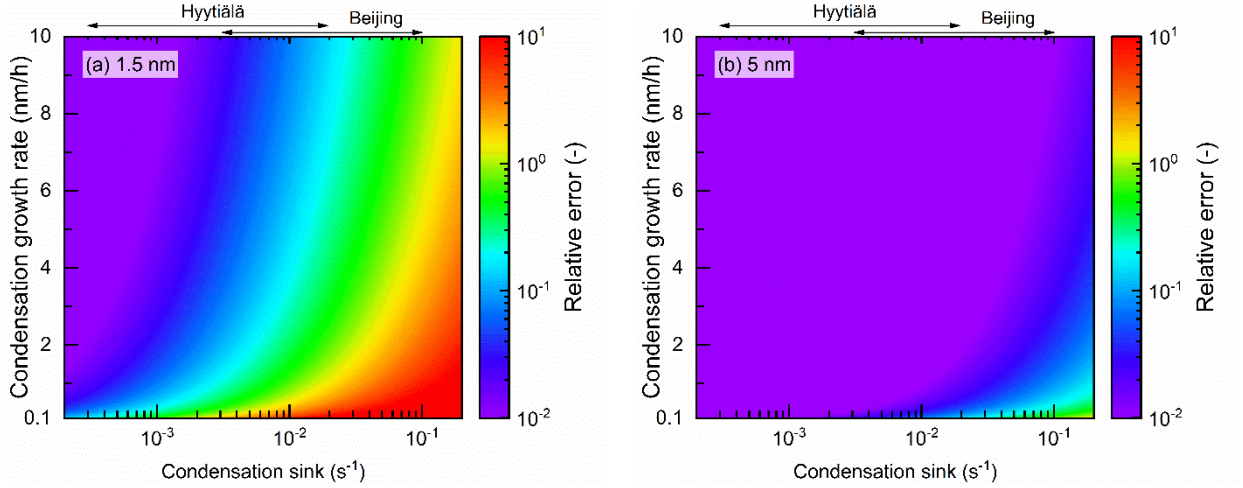

Figure A1 Error of the growth rate retrieved using the conventional appearance time method for (a) 1.5 nm and (b) 5 nm particles. The relative error is defined as $(GR_{conv}–GR_{cond})/GR_{cond}$, where GR_{conv} is the growth rate retrieved by the conventional appearance time method and GR_{cond} is the condensation growth rate. Coagulation growth is neglected in this figure. The approximate range of condensation sink in Beijing (Wang et al., 2013) and Hyytiälä (Dal Maso et al., 2002) are marked with arrows, which indicate the typical condensation sink in polluted and clean environments, respectively.